ANALYSIS OF THE LINDQUIST OCEAN WAVE FOLLOWER

John William Bonnett

NAVAL POSTGRADUATE SCHOOL
Monterey, California

THESIS

ANALYSIS OF
THE LINDQUIST OCEAN WAVE FOLLOWER

by

John William Bonnett

September 1975

Thesis Advisor: Noel Boston

Approved for public release; distribution unlimited.

Unclassified

SECURITY CLASSIFICATION OF THIS PAGE (When Data Entered)

REPORT DOCUMENTATION PAGE

READ INSTRUCTIONS BEFORE COMPLETING FORM

1. REPORT NUMBER	2. GOVT ACCESSION NO.	3. RECIPIENT'S CATALOG NUMBER
4. TITLE (and Subtitle) Analysis of the Lindquist Ocean Wave Follower		5. TYPE OF REPORT & PERIOD COVERED Master's Thesis September 1975
		6. PERFORMING ORG. REPORT NUMBER
7. AUTHOR(s) John William Bonnett		8. CONTRACT OR GRANT NUMBER(s)
9. PERFORMING ORGANIZATION NAME AND ADDRESS Naval Postgraduate School Monterey, California 93940		10. PROGRAM ELEMENT, PROJECT, TASK AREA & WORK UNIT NUMBERS
11. CONTROLLING OFFICE NAME AND ADDRESS Naval Postgraduate School Monterey, California 93940		12. REPORT DATE September 1975
		13. NUMBER OF PAGES 101
14. MONITORING AGENCY NAME & ADDRESS(if different from Controlling Office)		15. SECURITY CLASS. (of this report) Unclassified
		15a. DECLASSIFICATION/DOWNGRADING SCHEDULE

16. DISTRIBUTION STATEMENT (of this Report)

Approved for public release; distribution unlimited.

17. DISTRIBUTION STATEMENT (of the abstract entered in Block 20, if different from Report)

18. SUPPLEMENTARY NOTES

19. KEY WORDS (Continue on reverse side if necessary and identify by block number)

Lindquist Ocean Wave Follower

20. ABSTRACT (Continue on reverse side if necessary and identify by block number)

The Lindquist Ocean Wave Follower (LOWFER) is an electro-mechanical device which actively follows the sea surface. Although it measures waves, its primary purpose is to allow turbulence sensors to be placed near the naviface. Results of laboratory and field experiments are presented which demonstrate the degree to which the device can be used in the real environment. LOWFER has a maximum stroke of one meter, a tracking error of less than 7%, acceptable frequency response of up to 4 Hz, and is capable

DD FORM 1 JAN 73 1473 EDITION OF 1 NOV 65 IS OBSOLETE
(Page 1) S/N 0102-014-6601

Unclassified

SECURITY CLASSIFICATION OF THIS PAGE (When Data Entered)

20.
of carrying a 0.5 kg payload.

A second stage tethered catamaran/neutral buoyancy cylinder buoy was constructed and tested in conjunction with LOWFER. When LOWFER is used with the buoy, waves much larger than one meter can be followed. However, serious analysis problems are introduced into turbulence data taken in this manner.

Analysis of the Lindquist Ocean Wave Follower

by

John William Bonnett
Lieutenant, United States Navy
B.S.E.E., University of New Mexico, 1969

Submitted in partial fulfillment of the
requirements for the degree of

MASTER OF SCIENCE IN OCEANOGRAPHY

from the

NAVAL POSTGRADUATE SCHOOL
September 1975

ABSTRACT

The Lindquist Ocean Wave Follower (LOWFER) is an electro-mechanical device which actively follows the sea surface. Although it measures waves, its primary purpose is to allow turbulence sensors to be placed near the naviface. Results of laboratory and field experiments are presented which demonstrate the degree to which the device can be used in the real environment. LOWFER has a maximum stroke of one meter, a tracking error of less than 7%, acceptable frequency response of up to 4 Hz, and is capable of carrying a 0.5 kg payload.

A second stage tethered catamaran/neutral buoyancy cylinder buoy was constructed and tested in conjunction with LOWFER. When LOW-FER is used with the buoy, waves much larger than one meter can be followed. However, serious analysis problems are introduced into turbulence data taken in this manner.

TABLE OF CONTENTS

LIST OF FIGURES

To my Mother and Father.

ACKNOWLEDGEMENTS

I wish to thank Dr. Noel E. J. Boston for his generous guidance and support during my investigation. I would also like to thank Dr. Edward B. Thornton who provided me with invaluable assistance and motivation during all phases of the analysis and particularly for his assistance in the design of the second stage buoy.

I would like also to thank research technician Robert Smith for his instrumentation support, Hull Technician First Class Donald Antonacci and other machine shop personnel for their extraordinary work in constructing the catamaran/neutral buoyancy cylinder buoy, ship's master Woodrow Reynolds and crew of the R/V Acania and all other Naval Postgraduate School faculty and support personnel who provided assistance during this project.

I am also very deeply thankful to my wife Marsha and to my children, John and Stephanie. Without their cooperation and understanding I could not have completed this thesis.

I. INTRODUCTION

When a turbulent stream of air blows over an ocean surface, there is a resultant net transfer of energy. A knowledge of the structure of the turbulence in the layer immediately above the ocean surface is required to understand the mechanisms for this energy transfer [Shemdin and Lai, 1973]. In an effort to gain a greater understanding of these processes, investigators have mounted turbulence sensing instruments a fixed distance above the mean ocean surface. In most cases, they were unable to detect wave-induced turbulence partly because the sensors were required to be positioned rather high above the waves for protection.

Laboratory measurements of wind above waves generally give logarithmic velocity profiles when plotted against height. Some researchers (e. g. Shemdin and Hsu, 1966, 1967; Shemdin, 1967) have presented evidence that the velocity profile over the crest of a wave differs from that over a trough [Stewart, 1970]. A method to confirm or refute such theories would be to position sensors a fixed relative distance over all points of the wave profile. By using a wave follower, sensors can be synchronously moved with the changing wave profile and thus can be maintained at a constant elevation in the turbulent boundary layer.

A wave follower is a device that accurately and actively follows the vertical motions of an undulating water surface. The design of wave followers historically has been based on a feedback-control principle by which the vertical position of a water detecting sensor is maintained at a fixed relative position to the air-sea interface. The instrument should have a generally flat, linear response for the wave and turbulence scales of interest. The wave follower should not interfere with ocean processes such as the waves, wind velocity field across the waves or with the heat and momentum fluxes at the air-sea interface. In addition, it must be capable of carrying variety of sensors such as hot film anemometers, pressure sensors, and thermistors.

The accurate following of a wave profile in the field and to some extent in the laboratory is difficult. Several wave followers have been tried with varying success. Most mechanical wave followers do not have a stroke (the maximum wave height that can be followed) great enough to follow high amplitude sea and swell. Those that do are often of such proportions that they are unable to follow small scale wave structure and they interfere with ocean processes. Floats seem appropriate for high amplitude waves, but as a rule, they do not respond well to small structure. They also have a tendency to introduce heave and pitch motions which further complicate an already complicated picture.

Instrument induced error may or may not matter for a particular problem. A wave follower that only slightly distorted the true wave

profile would give average values of wave height, period, etc. which are acceptable in many studies. However, slight distortions could introduce spurious Fourier frequency components which may be of importance when studying non-linear phenomena such as turbulence. The researcher is understandably perplexed when trying to separate the instrument's "signature" from true environmental behavior [After Kinsman, 1970].

II. OBJECTIVES

The objectives of this research are:

1. To determine the capabilities and limitations of the Lindquist Ocean Wave Follower (LOWFER).
2. To compare LOWFER with other wave followers.
3. To adapt the LOWFER for use in the ocean environment.
4. To determine the capabilities and limitations of the two stage follower in the ocean environment.

III. DEVELOPMENT OF WAVE FOLLOWERS

A. GENERAL

The development of wave followers has been limited to designs which grew out of individual research projects. There has been no commercial effort to develop an instrument that might find general acceptance in the air-sea interaction field. As a result, several designs have evolved. Except for simple float devices, most employ some form of electro-mechanical feedback control.

B. PASSIVE SYSTEMS

One of the early designs for a wave follower was by Ramzy and Young [1968]. In their design, thermistors were mounted at various positions on a floating styrofoam hemisphere (figure 1). No error analysis regarding wave follower accuracy was undertaken. One of the more serious drawbacks to this type approach was the lack of a wave profile output representing the waves directly below the sensor.

C. ACTIVE SYSTEMS

1. Davis Wave Follower

Another early design of a wave follower was by Davis [1969] which operated on a feedback-control principle. An error signal was generated by the relative submersion of a resistance wave gage which

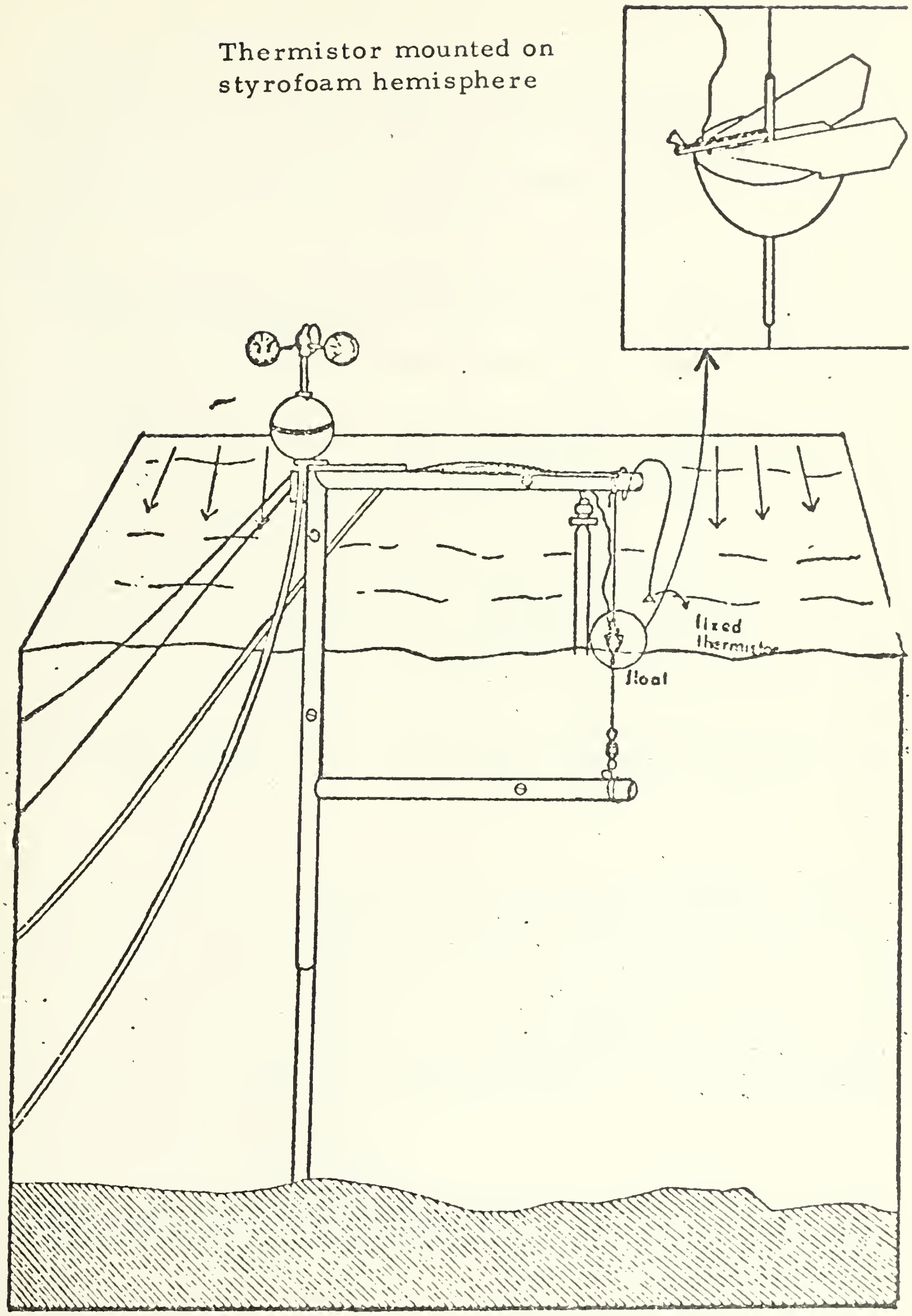

Figure 1. Float Wave Follower
(After Ramzy and Young, 1968)

was incorporated as one leg of a Wheatstone bridge. The resistance of the leg and hence the balance of the bridge varied with the depth of immersion. The error signal is fed to the servo amplifier which in turn provides a control voltage to the shaft-positioning servo motor (figure 2).

The arm assembly for the device is shown in figure 3. The arm and slide travel vertically on the track by means of a pulley arrangement driven by the servo motor. Two fully interchangeable arms are incorporated for either laboratory or field use. The shorter laboratory arm (9 inches in length) has a vertical travel up to 9 inches while the field arm (48 inches in length) can be used for much greater amplitude waves. Arm position output representing the wave profile is provided for by the potentiometer which is connected directly to the servo gear train.

The instrument was tested both statically utilizing a still water surface and synamically using mechanically and wind generated waves in a wave tank. The results indicated a rather optimistic 0.8mm maximum error over all wave heights and periods of interest. Accuracy measurements were not taken in the field.

2. Shemdin and Lai Wave Follower

A more recent design was developed by Shemdin and Lai [1973]. The wave follower is based again on the feedback-control principle in which the submergence of a wave height gage mounted on a moveable shaft is kept constant by following the moving water surface. The

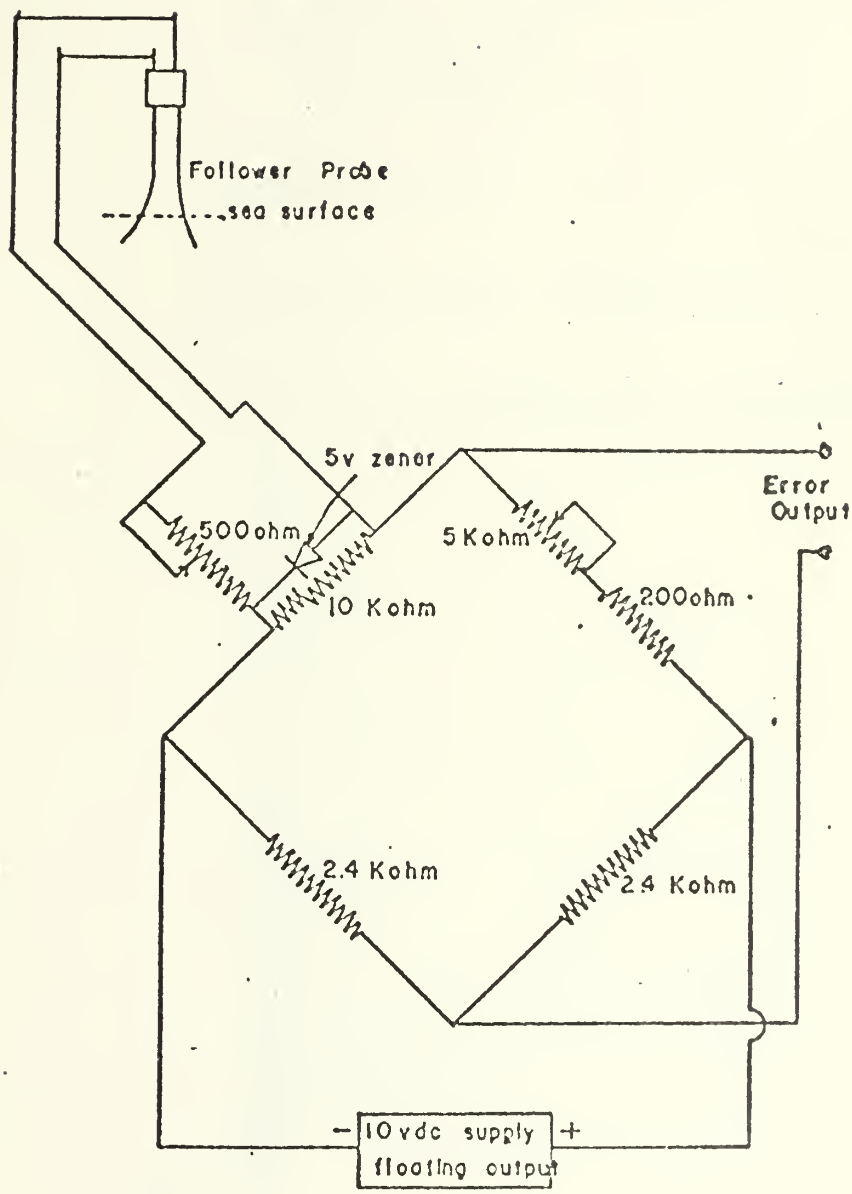

Figure 2. Wave Follower Error Circuit
(After Davis, 1969)

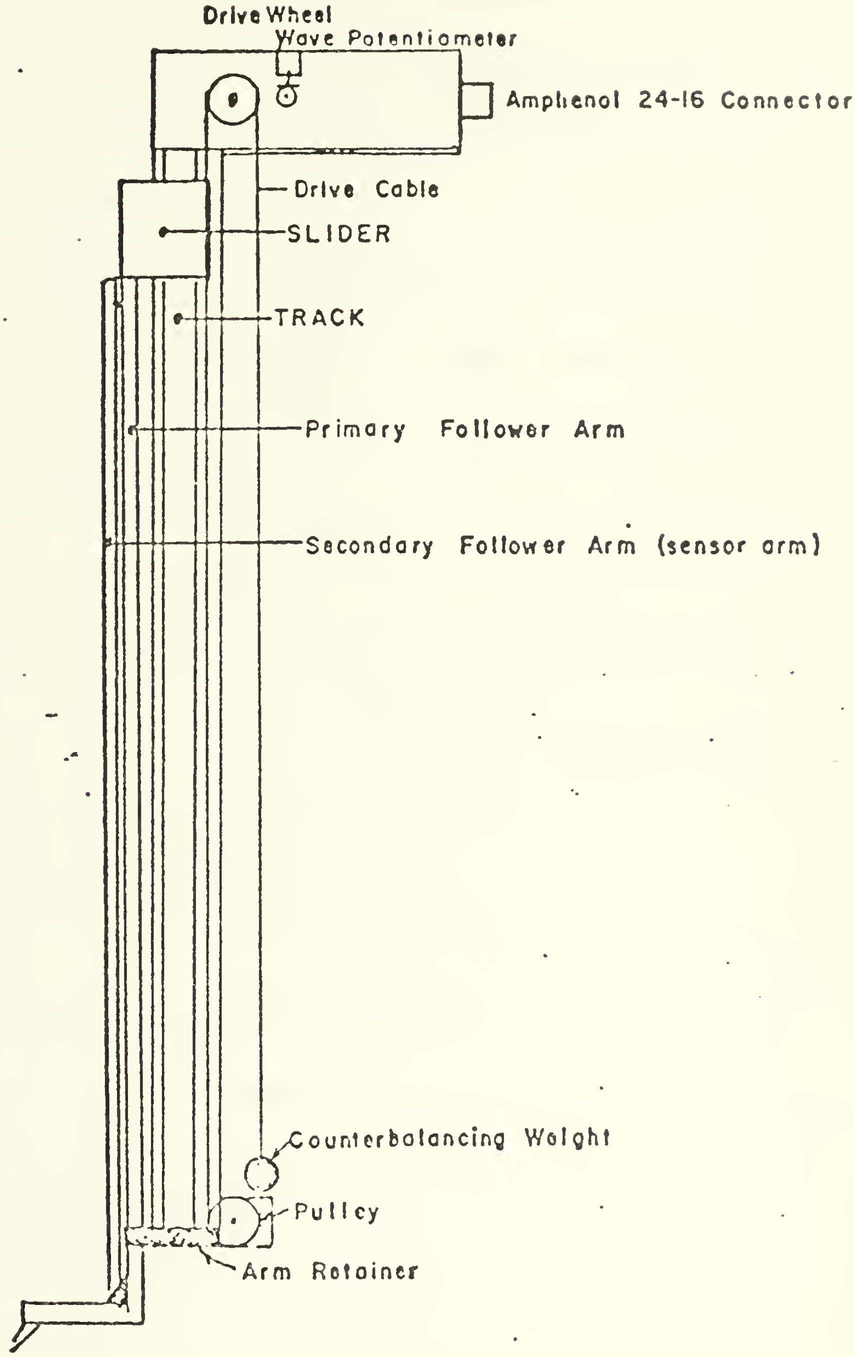

Figure 3. Wave Follower Arm and Mast Assembly
(After Davis, 1969)

mechanical system is shown in figure 4. A stainless steel shaft moves linearly up and down inside a larger steel cylinder. The dc motor is linked to the moving shaft by a pulley and cable mechanism. A smaller auxiliary motor is used for vertical traversing of the sensors. The wave follower normally carries an array of turbulence sensors and two wave gages. One wave gage provides an error signal to the drive motor while the other provides a displacement signal for the moving traverse mechanism with respect to the moving water surface.

A block diagram of the electronic system is shown in figure 5. The two stage (z and dz) vertical positioning can result in a $\pm$ 3% tracking error for a wave height of 10 cm and a frequency of 0.7 Hz [Shemdin and Lai, 1973]. Careful tuning and optimization are required however before the above specifications can be realized.

3. Additional Wave Follower Designs

The Chesapeake Bay Institute (CBI) wave follower (figure 6) is a two stage hydraulic and electro-mechanical system intended for wind wave generation studies in small amplitude wave areas [Peep and Flower, 1969]. It has a 30 cm stroke and a tracking accuracy that varies according to amplitude and frequency. Maximum tracking error (8%) occurs at 0.86 Hz and 30 cm wave height.

Dobson built a similar system which he used during the Joint North Sea Wave Project (JONSWAP II). His unit includes an additional tide compensating mechanism in order to insure maximum use of the hydraulic pistons stroke length.

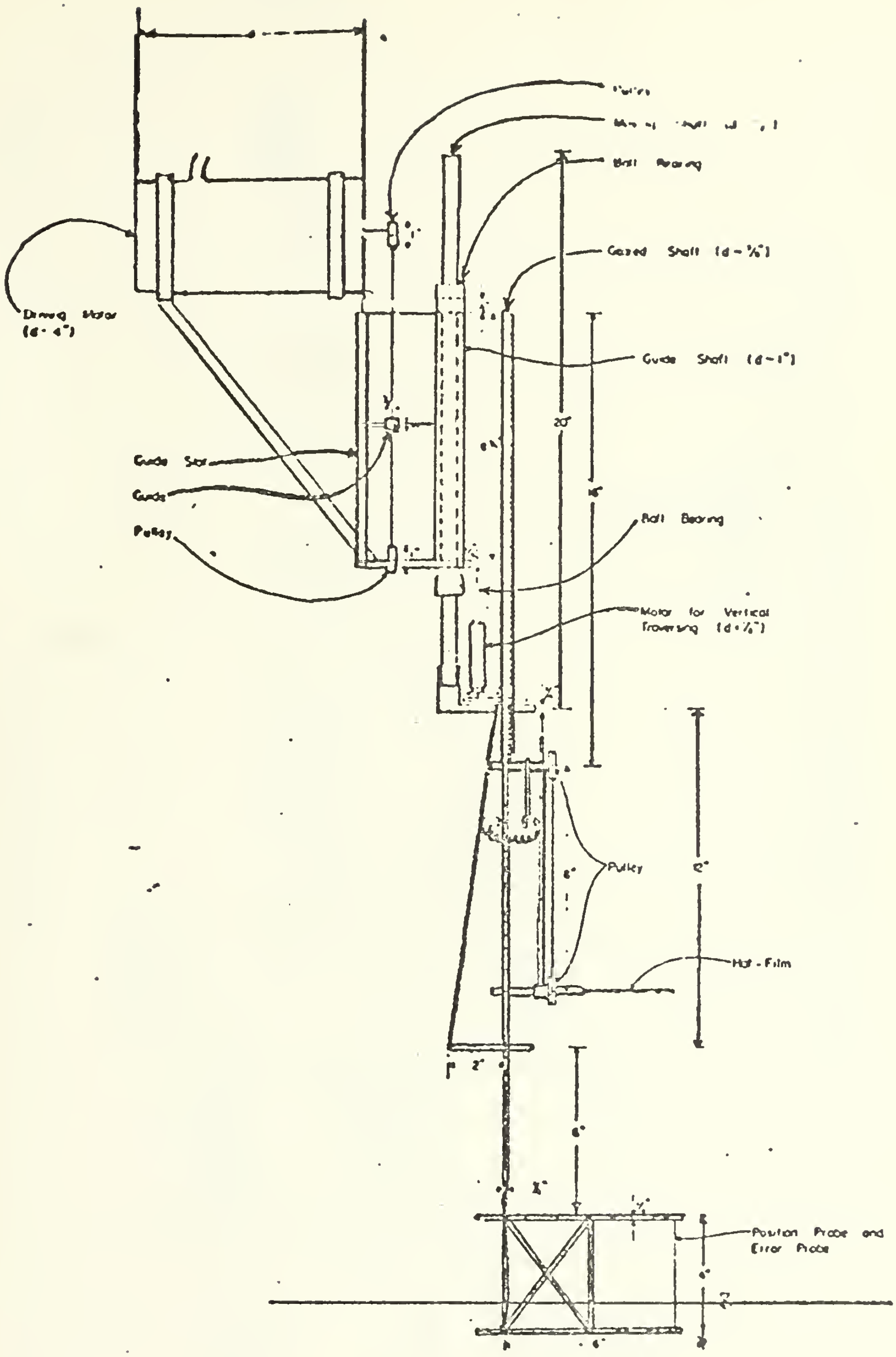

Figure 4. Wave Follower Traverse Mechanism
(After Shemdin and Lai, 1973)

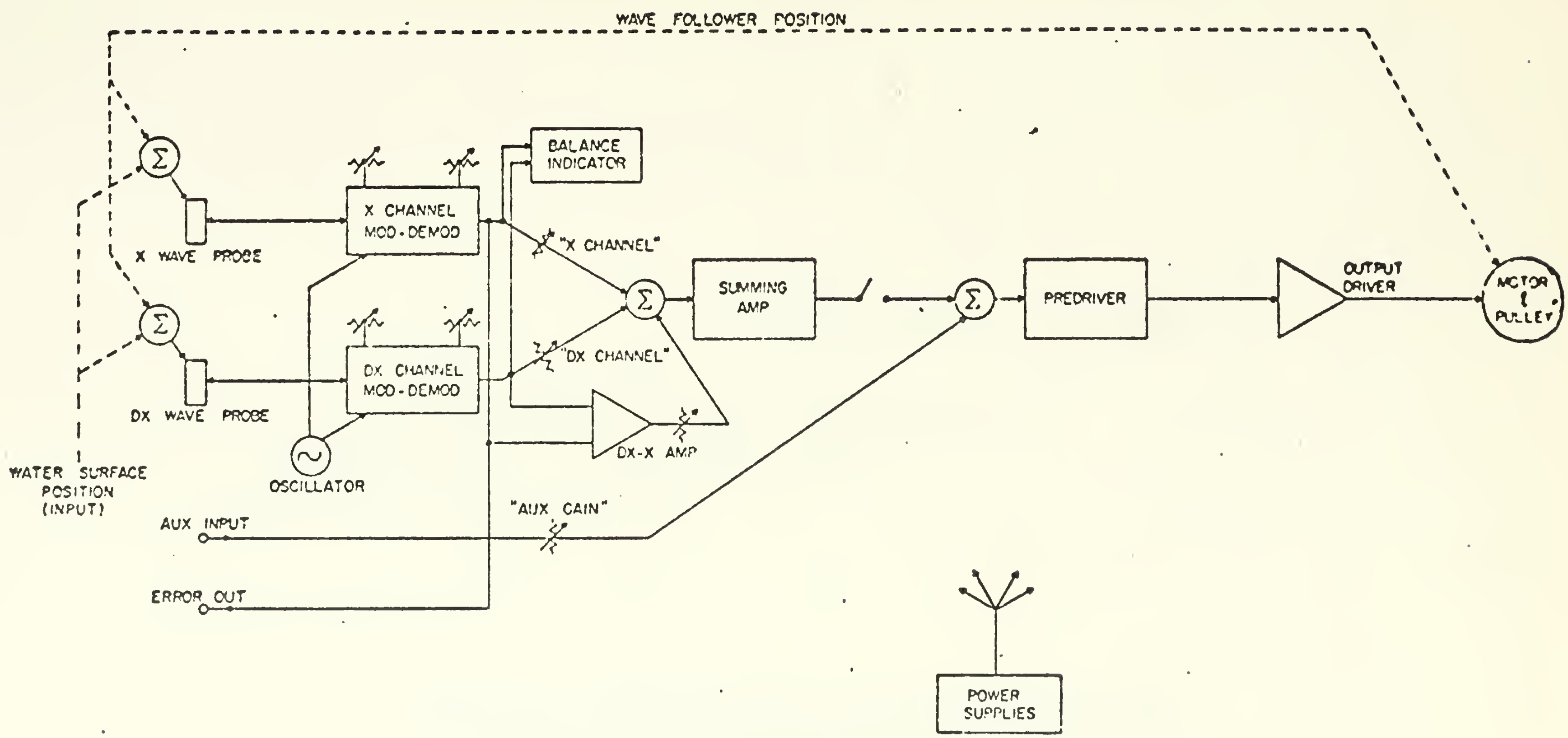

Figure 5. Wave Follower Electronic Block Diagram
(After Shemdin and Lai, 1973)

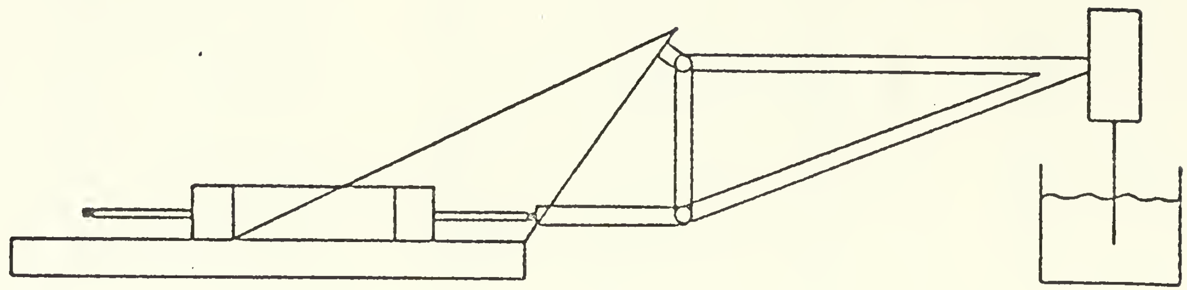

Figure 6. Chesapeake Bay Institute Wave Follower
Two Stage Hydraulic and Electro-Mechanical System
(After Peep and Flower, 1969)

The University of Florida wave follower is a hydraulic/electro-mechanical wave follower operated from beneath the water surface (figure 7). The system was designed to have a $\pm$ 3 cm relative vertical displacement. Maximum measurement condition is a crest to trough wave height of 1.8 meters.

D. LINDQUIST OCEAN WAVE FOLLOWER

1. General

The Lindquist Ocean Wave Follower is a device that is sensitive to the vertical motion of electrically conductive water. It is capable of carrying an array of sensors a fixed relative distance above a wavy ocean surface. The LOWFER is designed to have minimum interference with air-sea environmental processes and is capable of following a wide variety of wave conditions. The instrument has an essentially linear transfer function over the wave frequency and wave amplitude scales of interest.

The system was designed for use in the laboratory, but through additional modification, the system has been adapted for use in the ocean environment. In each configuration, the electronics are housed separately from the shaft positioning servo/probe sensor system. The electronic circuitry provides feedback and control information which is transmitted via a long multi-stranded cable between the shaft positioning servo and probe sensor unit. The dc servo motor direct drives the shaft by means of a rack and pinion arrangement.

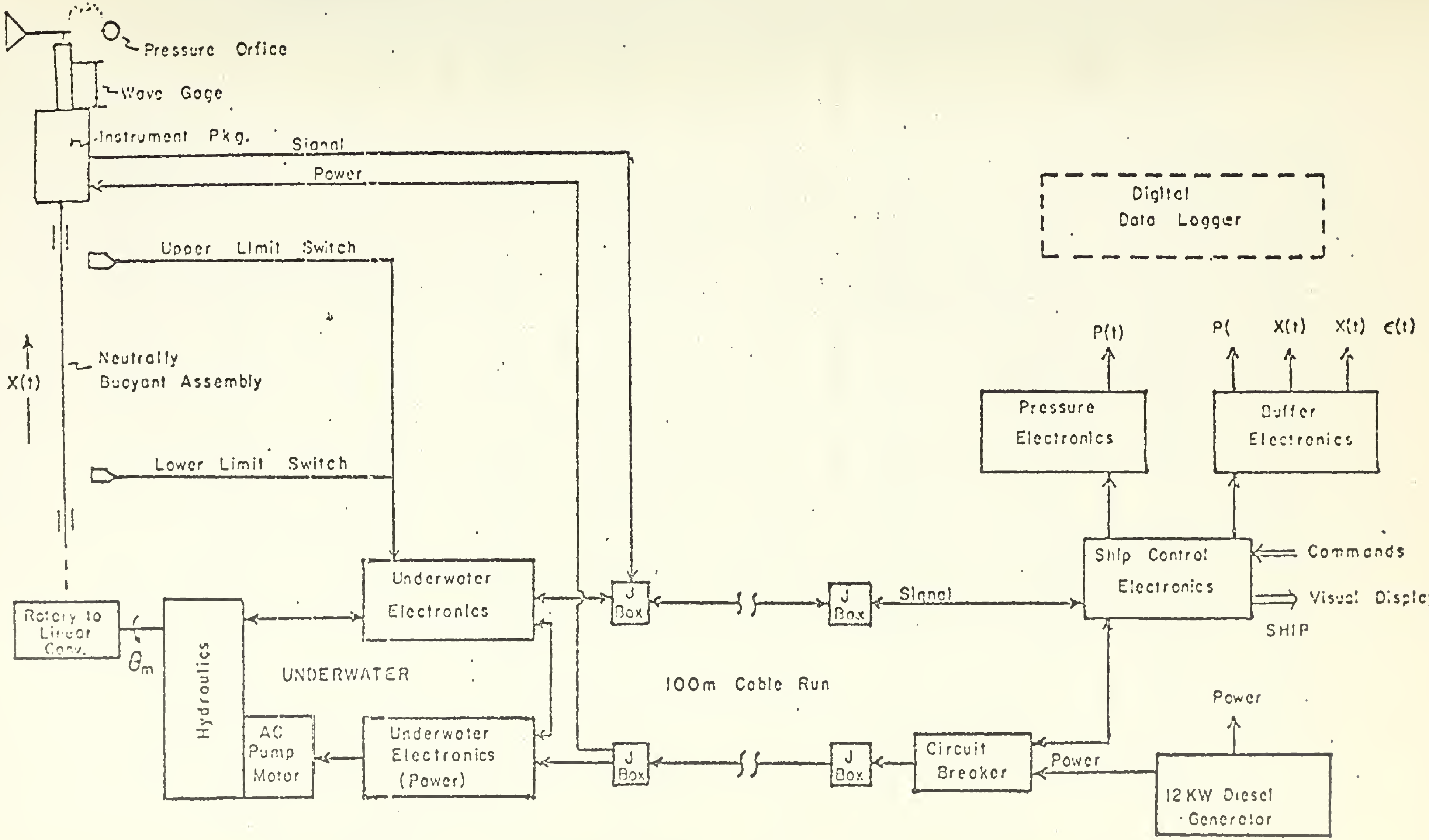

Figure 7. University of Florida Wave Follower System Block Diagram (After University of Florida, 1975)

2. Details

The Lindquist Ocean Wave Follower was developed under U. S. Navy Project No. 62271-4084-5773 by David Lindquist, 4648 West 14th Street, Vancouver, British Columbia, Canada. Design and fabrication closely followed a formal contract description and specification outline.

a. Contract Description and Specifications

The system is to be such that it can be operated just above and below the wave surface with sensors mounted to make crucial wave measurements including: (1) measurements in the air of the wave trough without being submerged during passage of the wave crest, and (2) measurements above the wave crest without being exposed during passage of the wave trough. It must be capable of following the waves.

The system should consist of a head (sensor system end), a connecting cable and a panel end (output). The head must be able to be mounted from surface penetrating buoys, towers, pilings, etc.. Its weight should not exceed 10 kg. The head assembly must present a small profile to the wind, not to exceed 2.5 m in length and 12 cm in depth. The panel meter section should be capable of facilitating equipment adjustment and use. The connecting cable is to be shielded and capable of operating in sea water. In addition to the general specifications, the following technical requirements are imposed: (1) total excursion of the surface sensing element should be at least 2 m, (2) the shaft should move with a maximum velocity of 1.2 m/sec.,

(3) the shaft should have a travel rate capable of making eight complete up and down 5 cm excursions in one second, (4) perturbation area to the wave front should not exceed 1 cm^2, (5) all parts in contact with the sea water should be made of stainless steel, (6) the head system should operate in waters with salinity ranging from 3‰ to 40‰, (7) additional sensors should be able to be attached to the sensor arm, (8) total payload be at least 0.5 kg.

b. Physical Description of LOWFER

The appearance and physical size of the laboratory version of LOWFER are shown in figure 8. The electronic components are mounted on plug-in type boards attached to a copper chassis. The shaft and shaft-positioning servo motor along with bearings and shaft connections are mounted on a plexiglass support.

c. Electronic Circuitry of LOWFER

A block diagram of the LOWFER electronic circuitry is shown in figure 9. In the functional description which follows, key circuit names are underlined.

1. The <u>oscillator</u> is a free running multivibrator and supplies two simultaneous outputs -- a reference signal and an error signal.
2. The <u>reference balance circuit</u> is used to match the the reference signal to the conduction condition of the error modulator.

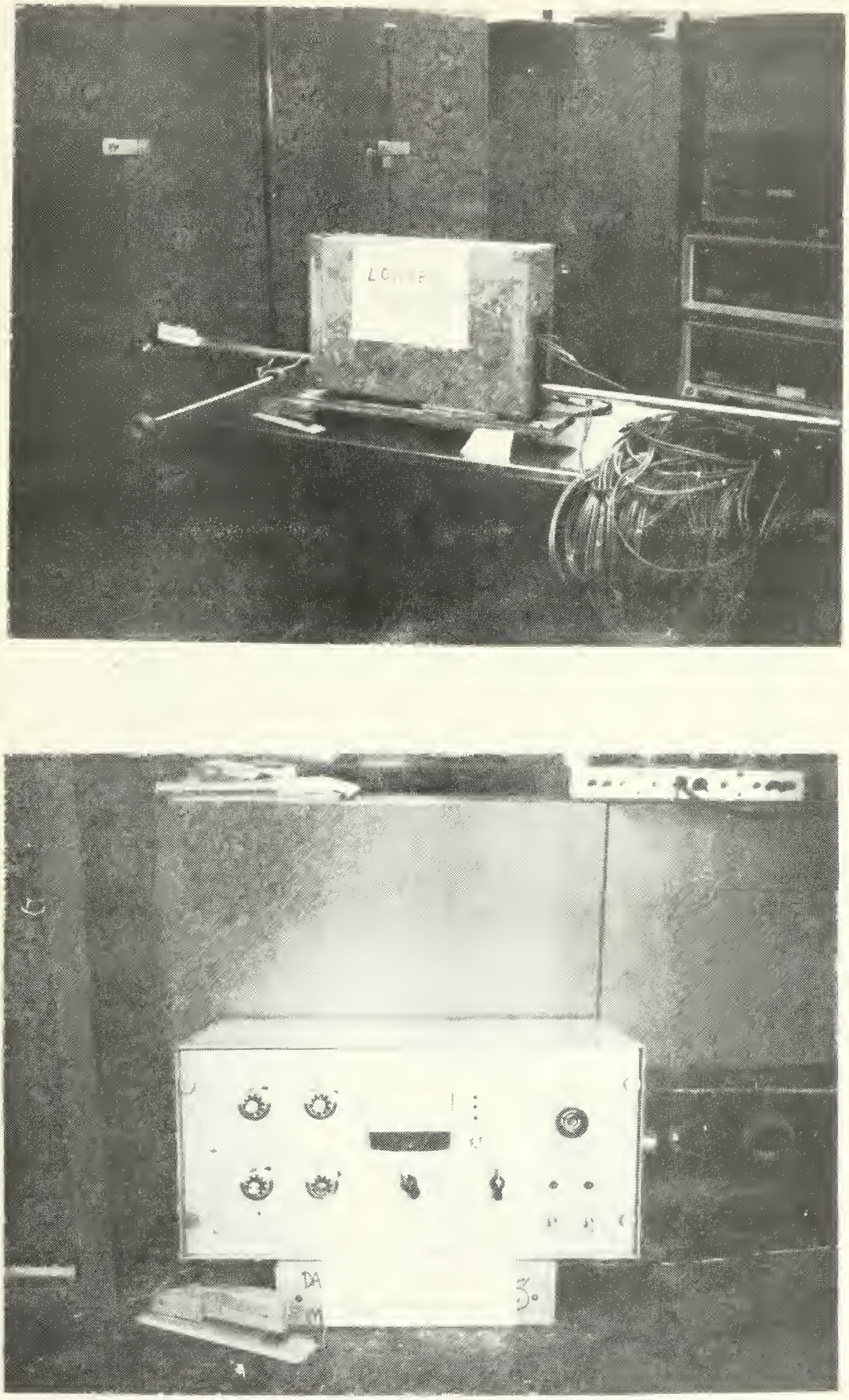

Figure 8. LOWFER, Laboratory Configuration

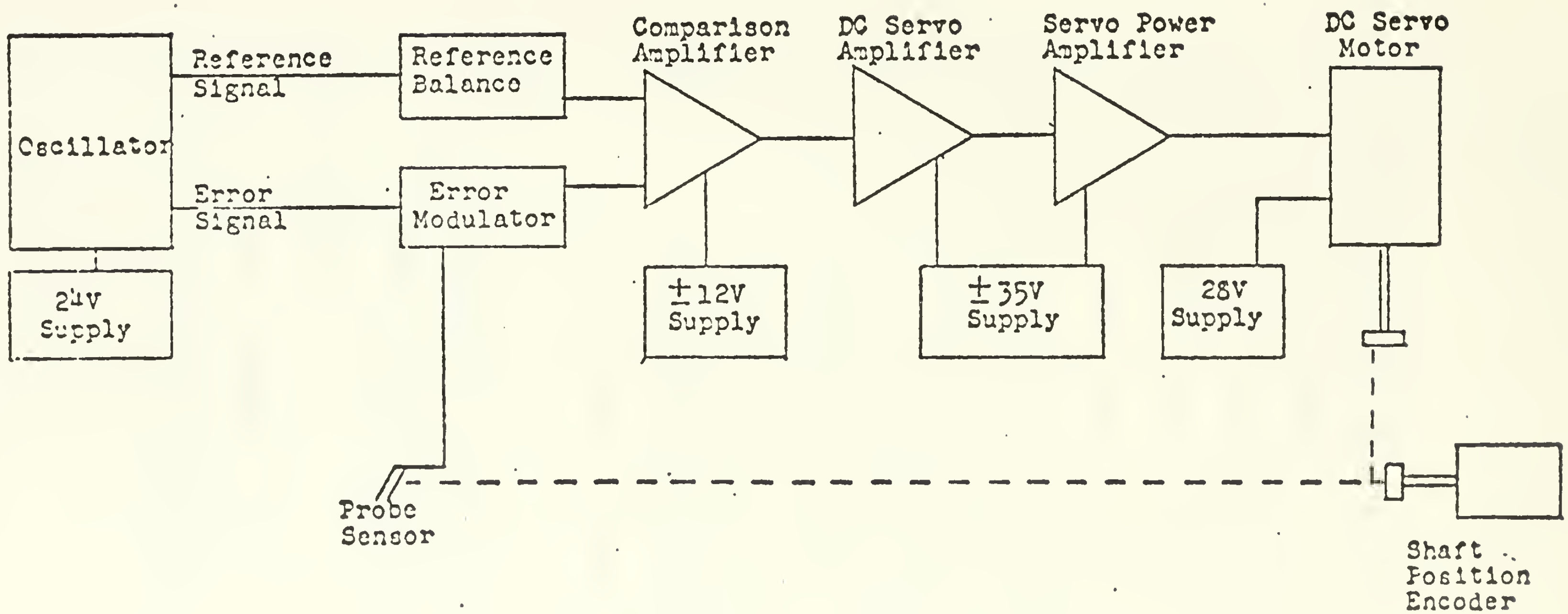

Figure 9. Lindquist Ocean Wave Follower Electronic Block Diagram

3. The error modulator modulates the error signal in accordance with the water conductivity at the probe sensor.

4. The comparison amplifier circuit receives input signals from the reference balance and error modulator circuits. Each input is converted from an alternating voltage to a direct voltage. The dc reference signal is set to the desired value by means of a reference adjust control. The dc error signal is set to a corresponding level by the error adjust control. Both dc signals are fed to a dc amplifier which amplifies the difference between the two signals. This results in an output from the amplifier that is either positive, negative, or null depending on whether the error signal is greater than, less than or equal to the reference signal.

5. The dc servo amplifier accepts the comparison amplifier and amplifies it sufficiently to drive the servo power amplifier.

6. The servo power amplifier receives the composite signal from the dc servo amplifier and amplifies it to drive the dc servo motor which is geared to the shaft probe sensor combination.

7. The shaft position encoder is a potentiometer geared to the shaft and forms two legs of a Wheatstone bridge circuit. It provides the output signal for recording the wave profile.

d. Detailed Circuit Descriptions

(1) Oscillator and Motor Field Supply.

The oscillator and motor field supply is schematically represented in figure 10. The oscillator is a unijunction transistor multivibrator. The 3k-ohm resistor along with the 0. 1 μfd capacitor establish the fundamental oscillator frequency at approximately 1700 Hz. The oscillator drives a 2N497 NPN and a 166E36 transformer combination for each of the two output signals. The motor field supply supplies voltage to the field windings of the shaft drive motor. The circuit supplies a nominal output voltage of 30 volts. The Fairchild UA78M24 is an integrated circuit voltage regulator which acts as a buffer stage between the field supply and the oscillator circuit. It also supplies +24vdc to the oscillator.

(2) Reference Balance and Error Modulator

The reference balance and error modulator circuit is shown in figure 11. The reference balance circuit balances the error signal and the reference signal prior to modulation. The reference balance control is a potentiometer used for this purpose and is set for a desired probe depth. The error modulator circuit modulates the input

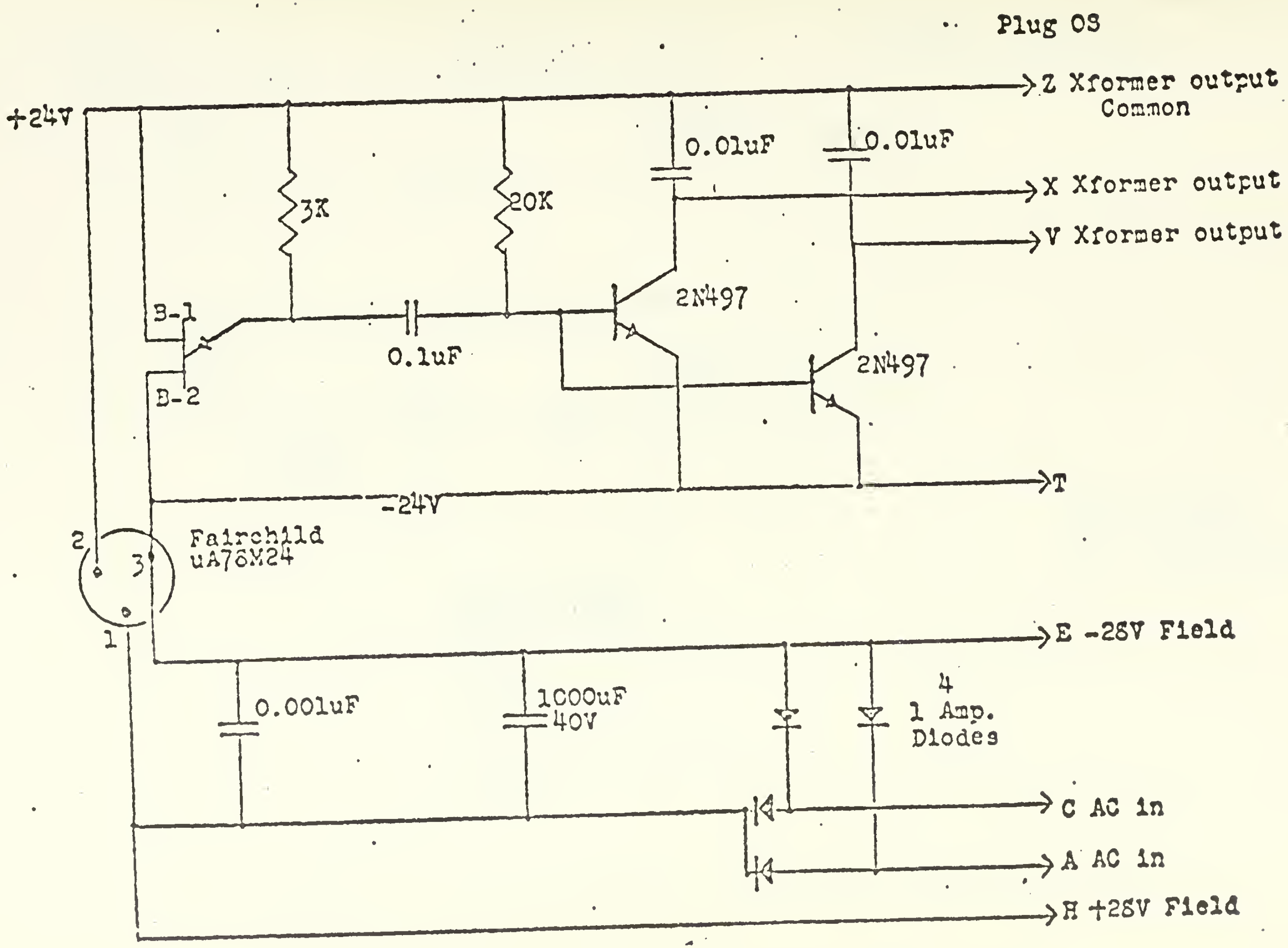

Figure 10. Oscillator and Motor Field Supply

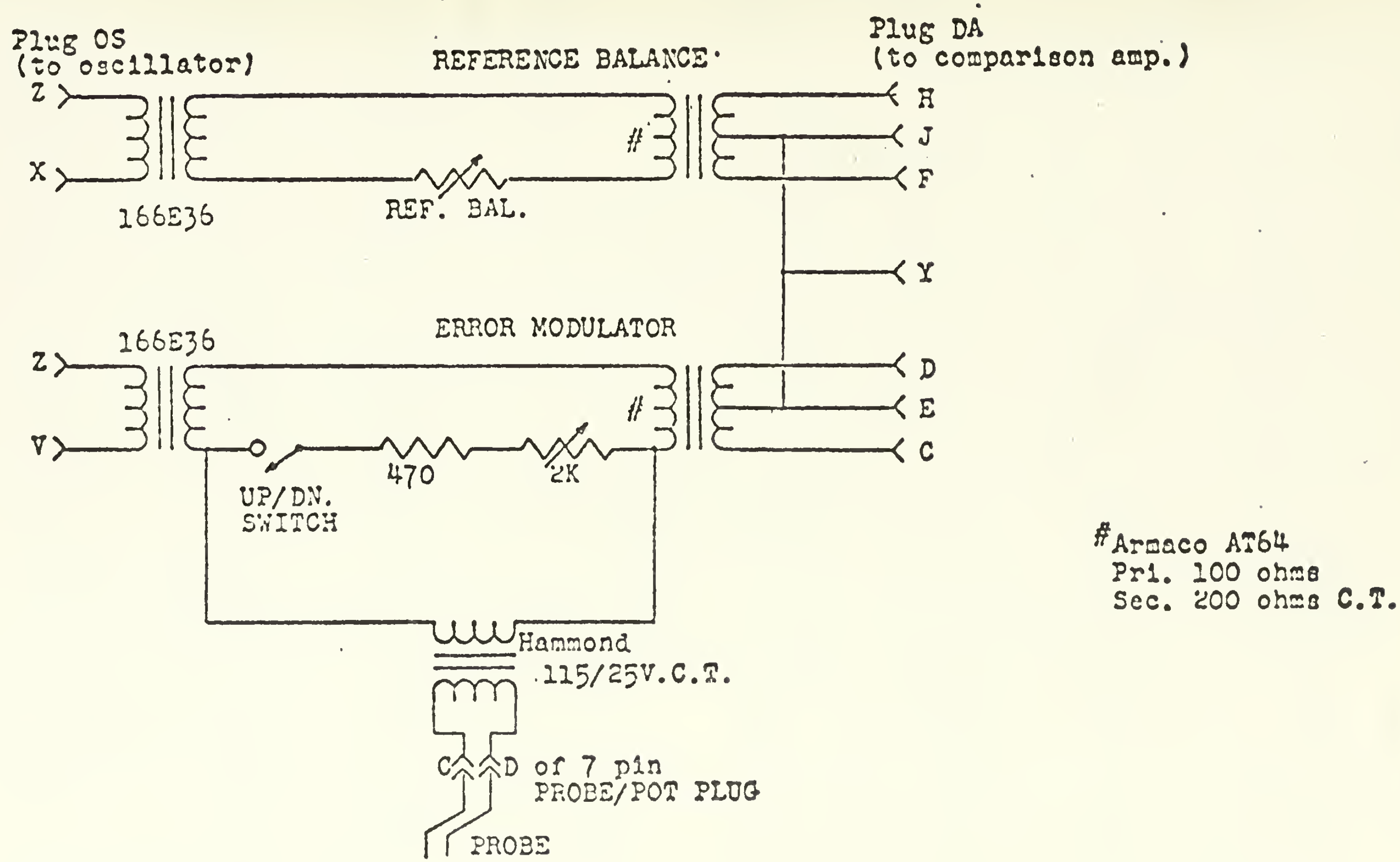

Figure 11. Reference Balance and Error Modulator Circuit

error signal in accordance with the varying conduction between the probe tips as a result of a slight change in probe depth. Increased penetration causes a corresponding reduction in amplitude. The modulator section also isolates the probe from remaining wave follower circuitry thus eliminating ground-loop conditions. The up/dn switch and probe impedance control (2 k-ohm pot.) are aids in controlling the shaft remotely while deploying or retrieving the probe from the water surface. This action is accomplished by artificially increasing the apparent probe depth causing an error signal to be generated and the shaft to withdraw. The probe impedance control and up/dn switch should not be used for more than about 15 seconds at a time as excessive heating can result in the power transistors of the servo motor driving circuits.

(3) Comparison Amplifier Circuit

The comparison amplifier circuit is shown in figure 12. The circuit has as its input the reference signal (constant amplitude) and the error signal (varying amplitude). The two signals are rectified and filtered and then reduced in amplitude by the reference adjust and error adjust potentiometers from 10 to 15 volts down to 0.1 to 0.2 volt range. Front panel switch positions (Rev V and Error V) sample voltage at the center tap of the potentiometers. The adjusted signals are then fed to separate inputs of the UA741 integrated circuit amplifier. This amplifier compares the error signal to the reference signal. If the error signal is less than the reference signal, the drive motor raises the

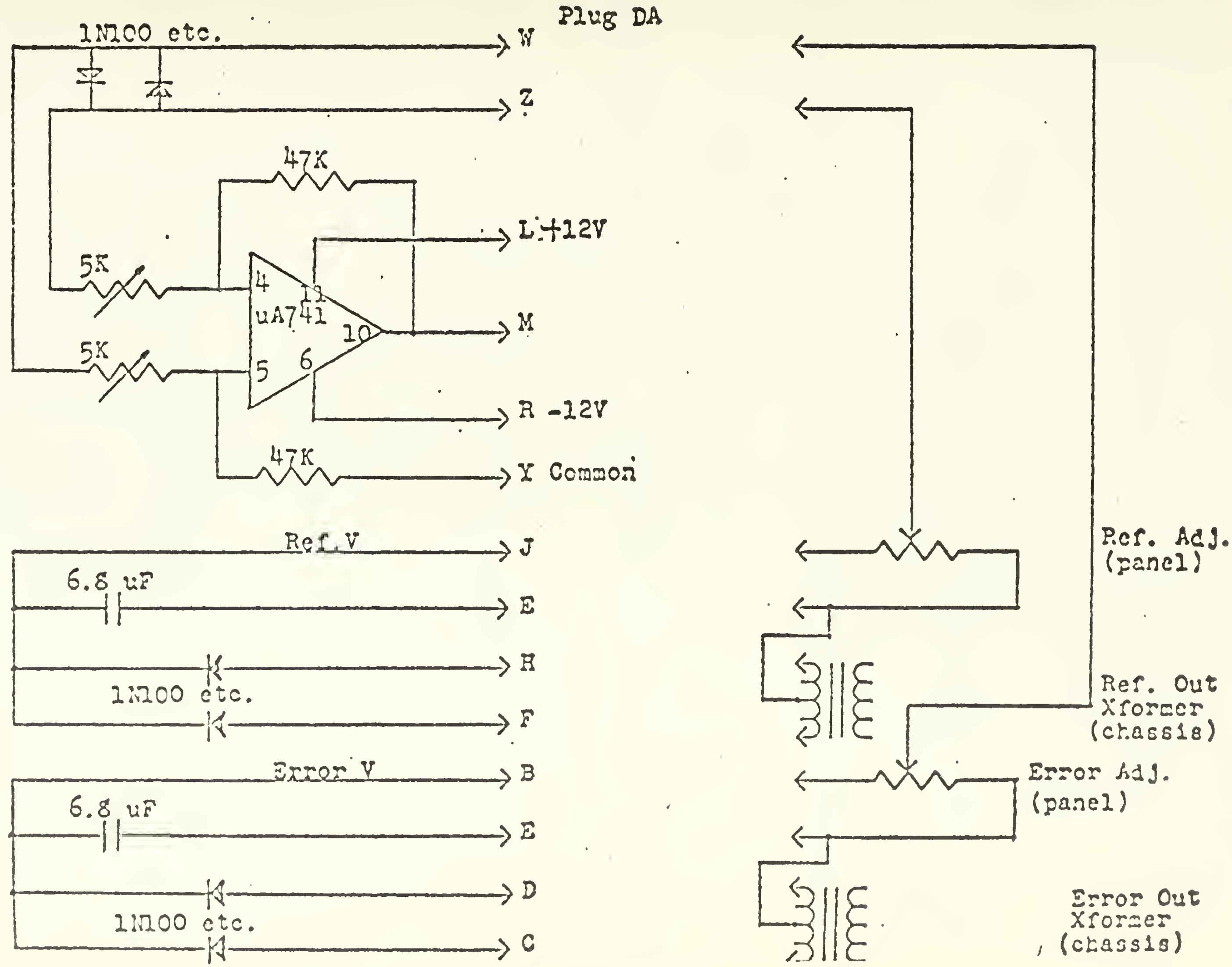

Figure 12. Comparison Amplifier Circuit

shaft. The diodes connected across the inputs to the integrated circuit serve as an automatic shunt that prevents overdriving of the amplifier. They will conduct at voltages greater than 0.75 volts. The variable 5 k-ohm potentiometers in the amplifier are adjusted to give the circuit a voltage gain of 15.

(4) D.C. Servo Amplifier Circuit

The d.c. servo amplifier increases the voltage level of the low voltage d.c. difference signal from the comparison amplifier. The amplified signal of between ± 30 volts is used to drive the servo power amplifier (figure 13).

The input stage consists of a pair of 2N930 transistors forming a differential amplifier. The input signal from the comparison amplifier is applied through a resistive network to one of the transistors, while a feedback signal from the servo power amplifier is applied to the other. The voltage divider network, consisting of the 10 k-ohm and the 470 k-ohm resistors, establishes the voltage gain of the servo amplifier at approximately 22. The transistor 2N3904, diode 1N735 and the 2 k-ohm and 2.7 k-ohm resistor combination form a constant current source in the emitter circuit of the differential amplifier thus improving stability. The output of the differential amplifier is fed to the transistor amplifier containing two 2N3905 transistors. The 0.1 μfd. capacitor and the 300 ohm resistor are used for circuit stability.

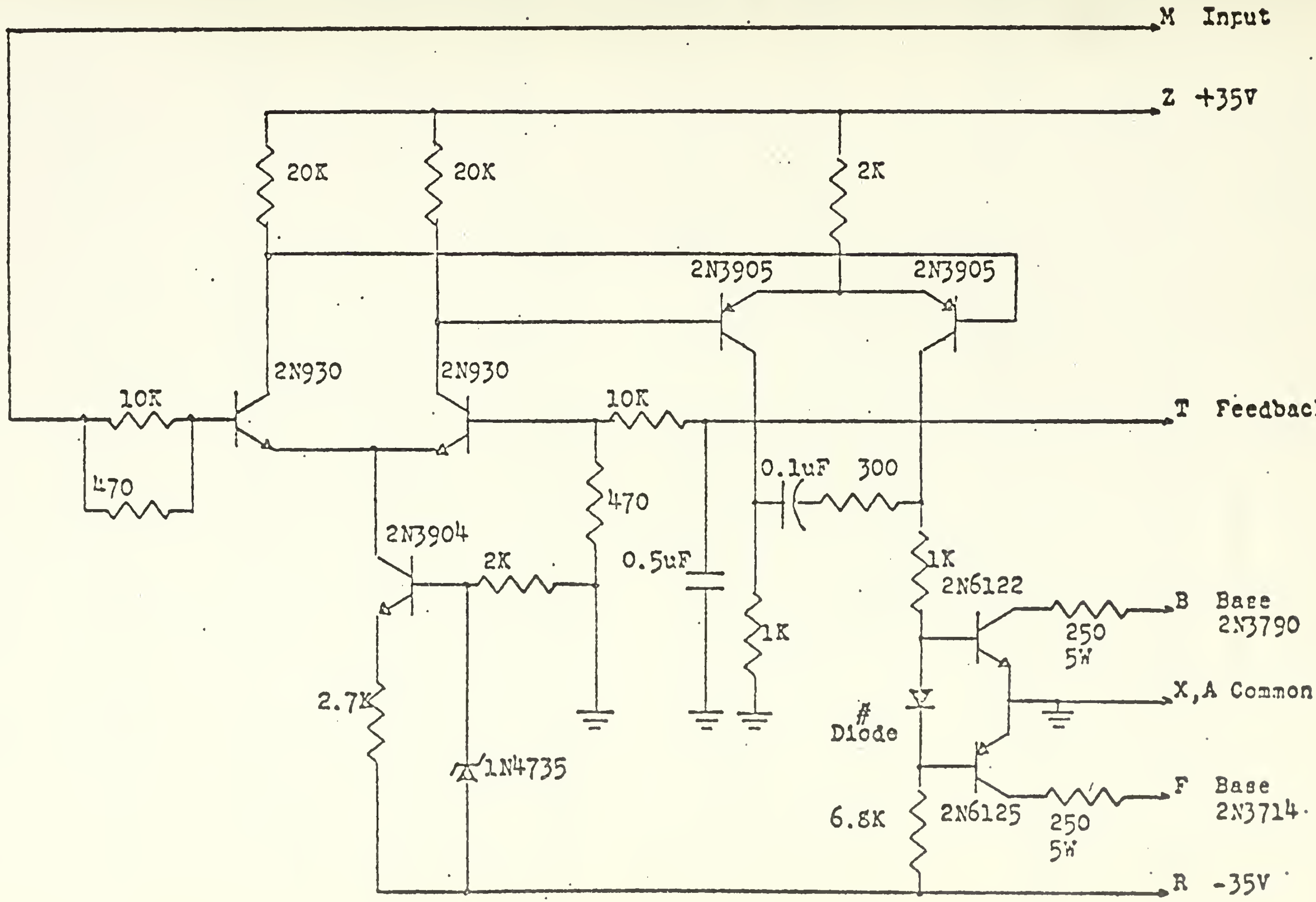

Figure 13. D. C. Servo Amplifier Circuit

The diode connecting the bases of the 2N6122/2N6125 pair provides forward bias voltage to drive the pair into conduction. The choice of the diode is critical since a higher forward bias voltage would cause over-conduction and heating while, in the opposite case, too little forward bias would cause a zero cross-over gap resulting in erratic action near the null position. The collector outputs from the 2N6122/2N6125 pair are used to drive the servo power amplifier.

(5) D. C. Servo Power Amplifier

The schematic diagram of the d. c. servo power amplifier is shown in figure 14. The servo power amplifier is an emitter follower used for impedance matching, isolation and for supplying a power gain to the servo motor. The circuit is housed in an oil tank for heat dissipation.

Ideally, only one transistor will be conducting at a given time depending on which way the motor is being driven. If the motor is holding the shaft in a steady position, as would be the case in still water, only the up driving transistor will be conducting to support the weight of the shaft and any load. In this condition, the transistor is in a steady mid-range conduction state requiring the greatest heat dissipation. Wave action causes the output transistors to work alternately so they are not generally in the mid-range condition as long with a corresponding lower overall heat production. The thermistor shown in the oil cooling tank is used for temperature sensing. Readout can be

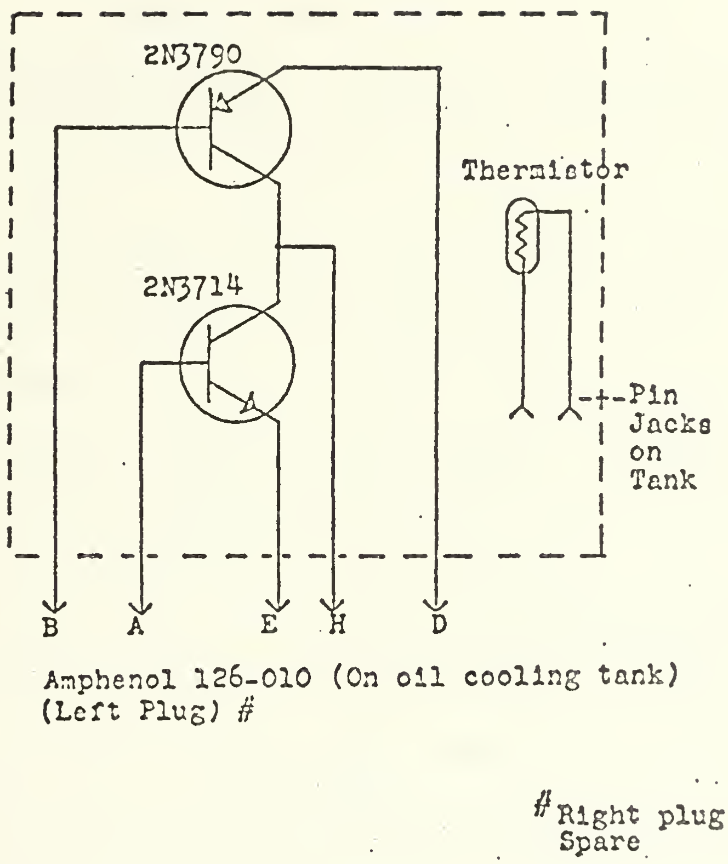

Figure 14. D. C. Servo Power Amplifier Circuit

accomplished by selecting the Driver T position on the function switch on the front panel.

(6) Shaft Position Readout Circuit

The shaft position readout circuit is shown in figure 15. It is a Wheatstone bridge circuit formed with two 10-turn 1000 ohm potentiometers. One potentiometer control is on the front equipment panel labeled Reference Zero Set. The other is the shaft encoder potentiometer on the motor/shaft drive chassis. The circuit is constructed so that the panel control setting is the zero point and the shaft encoder position will then give a signal at the Record Out terminals depending on the shaft position throughout its 100 cm range with respect to the point set by the panel control setting. If, for example, the Reference Zero Set control is set at 5 turns (half of the total number of turns available), then when the shaft is at the 50 cm position, the Record Out voltage will be zero and will have ± 5 volts at each end of travel. If the Reference Zero Set is set at zero turns, the Record Out would be 0 volts when the shaft is fully extended and 10 volts when the shaft is fully depressed. The Record Out variable potentiometer is used as a voltage divider to adjust output amplitude. The 2 k-ohm potentiometer is used to obtain a center voltage for metering either the Shaft Position or the Record Zero position. The meter gives an indication of the setting of the Record Zero control in the Record Zero function switch position. The Shaft Position setting of the function switch gives the position of the shaft with respect

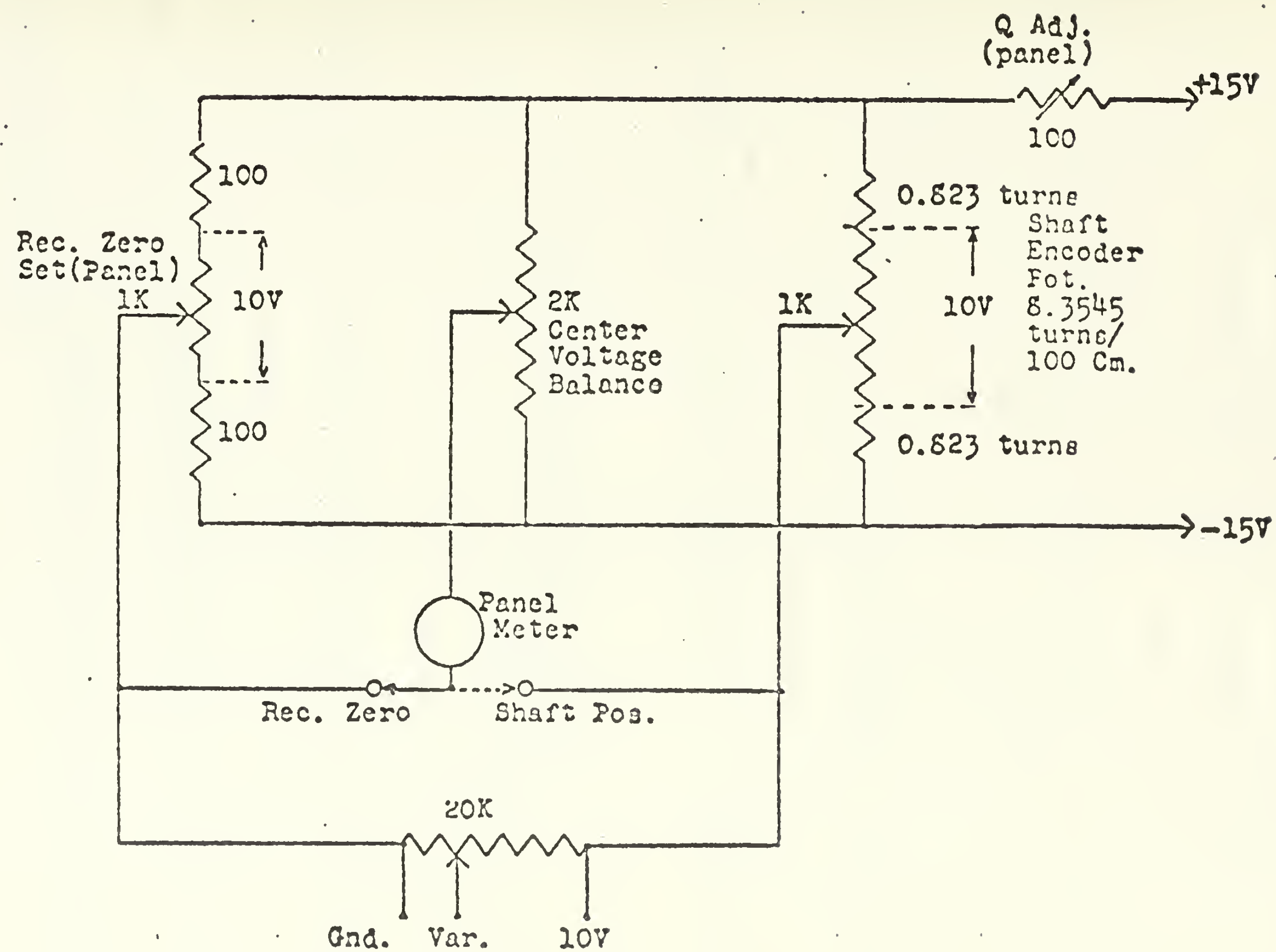

Figure 15. Shaft Position Readout Circuit

to the midpoint of shaft travel. The Q Adjust potentiometer reduces 15 volt supply voltage to 10 volts and compensates for wiring losses.

(7) Shaft Position Power Supply and Temperature Indicator

The shaft position power supply and temperature indicator circuits are shown in figure 16. The shaft position circuit receives 15 volts regulated by a Fairchild 7800M15 integrated regulator circuit. The temperature indicating circuit is a Wheatstone bridge comprised of a 2 k-ohm potentiometer, a fixed 1 k-ohm resistor, and a thermistor located in the d. c. servo power amplifier output transistor oil cooling tank. The 2 k-ohm potentiometer was adjusted for a zero meter reading when the thermistor was at 0° C. A regulated 1.2 volts is supplied to the circuit.

(8) Meter and Selector Switch Circuits

The meter and selector switch circuits are shown in figure 17. A photograph of the control panel is shown in figure 18. The operational and power supply monitoring positions can be useful in checkint for proper circuit operation or circuit malfunction.

1. The Driver V position gives an indication of the voltage level and polarity present at the servo motor.

2. The 35V position is a measurement of both plus and minus servo power supplies in series. Thus the voltage being monitored is approximately 70 volts.

3. The 12V position monitors the + 12 volts supplied to the comparative amplifier.

4. The 24V position monitors the regulated 24 volts used for the oscillator circuit.

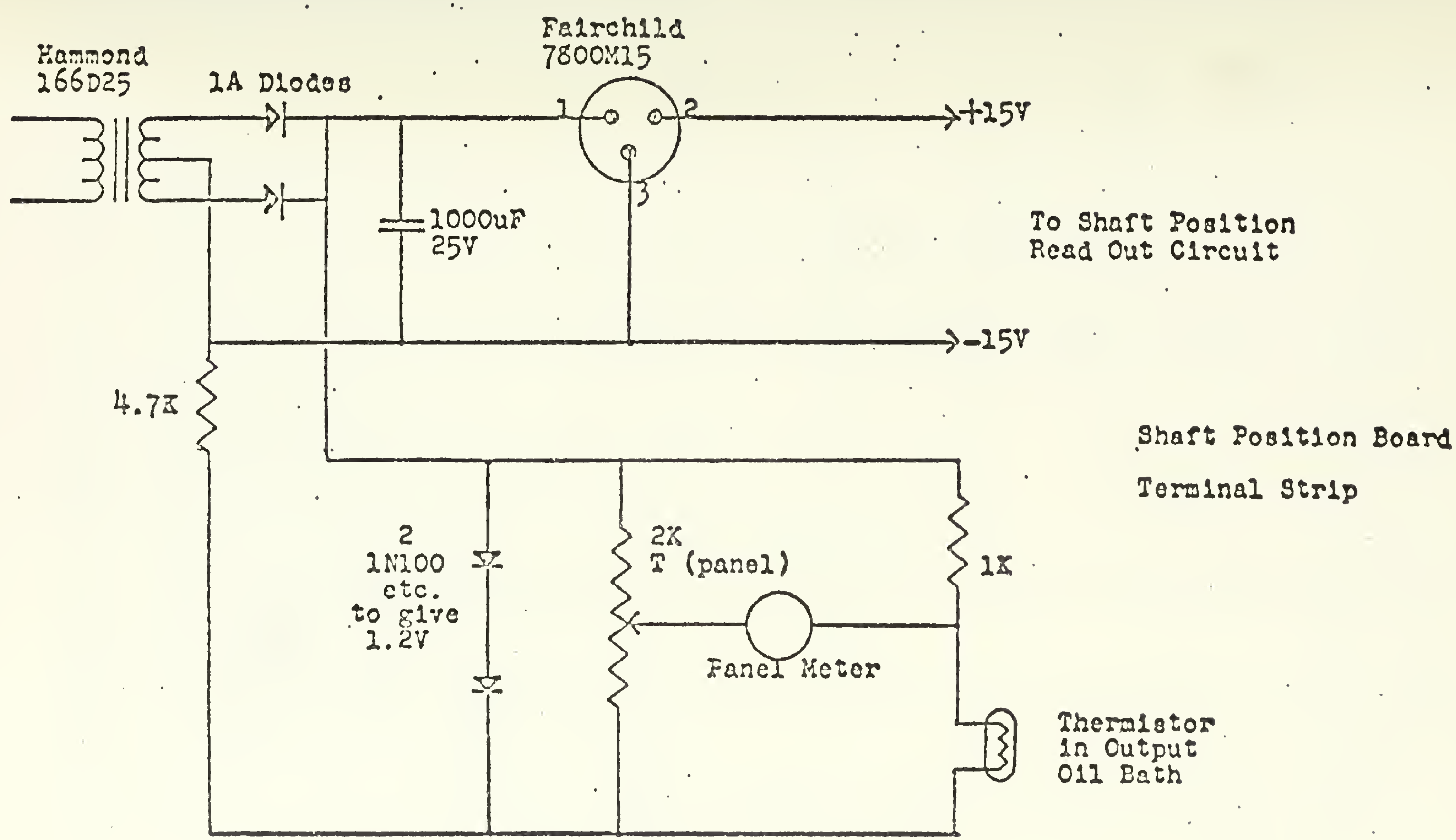

Figure 16. Shaft Position Power Supply and Temperature Indicator

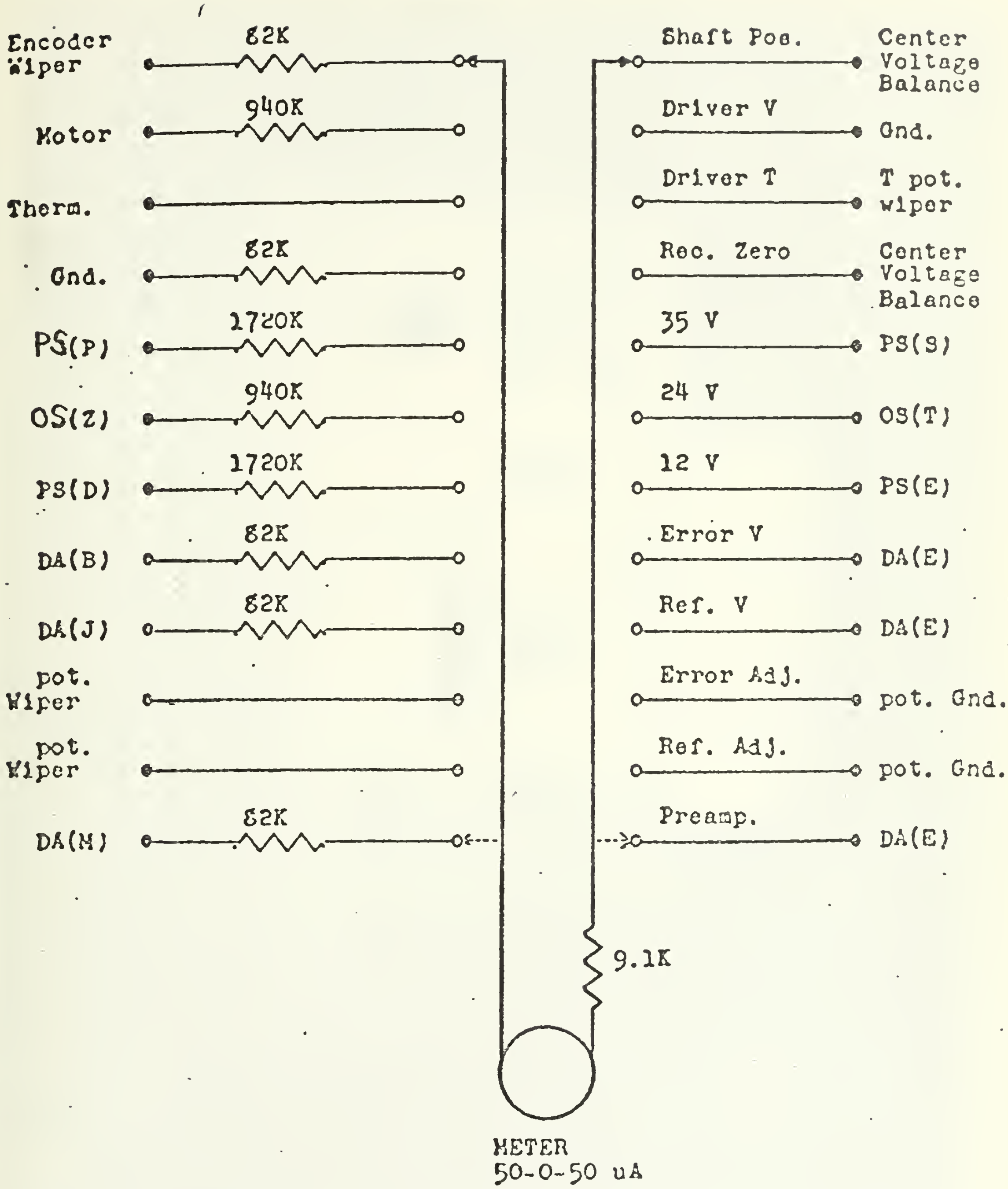

Figure 17. Panel Meter and Selector Switch Circuits

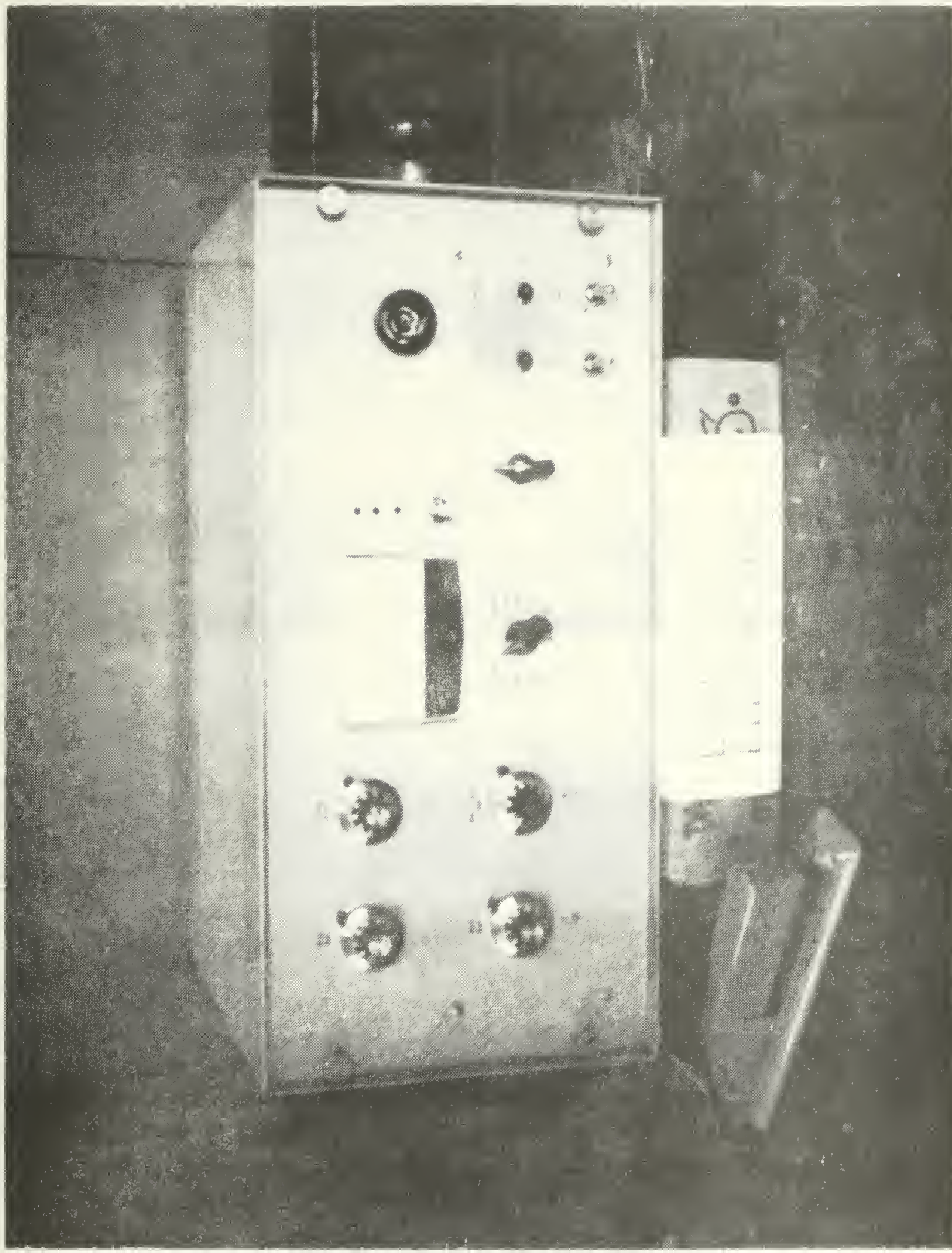

Figure 18. LOWFER Front Panel Configuration

5. The Error Adjust and Reference Adjust positions have a full scale reading of 50 and, when occurring, indicate 0.5 volts actually present.

6. The Preamp position full scale reading on the meter represents 5 volts actually present.

7. The Shaft Pos./Rec. Zero position is a voltage indication of shaft position.

8. The Driver T position indicates the oil bath temperature of the servo power amplifier circuit.

9. The Error/Ref. Voltage position has a scale conversion of 10 to 1 such that 50 represents 5 volts.

(9) Tachometer Output Circuit

The tachometer output terminal at the rear of the cabinet is connected directly to the tachometer generator on the drive motor. The signal may be used for special wave studies. The signal is an indication of the vertical acceleration of the shaft assembly. The output will be zero at the motor and shaft null or turnaround points and maximum (about 30 volts) when the shaft is traveling at full velocity.

(10) Power Supplies

The two power supply circuits are contained in figure 19. Both employ a full wave bridge rectifier with capacitive filtering. Voltage regulation is accomplished as necessary on the individual circuit boards. Voltage outputs for the two power supplies are $\pm$ 35 and $\pm$ 12 volts.

(11) Wiring Diagrams

Wiring diagrams for plugs and circuit boards are shown in figures 20, 21, 22, 23, 24 and 25.

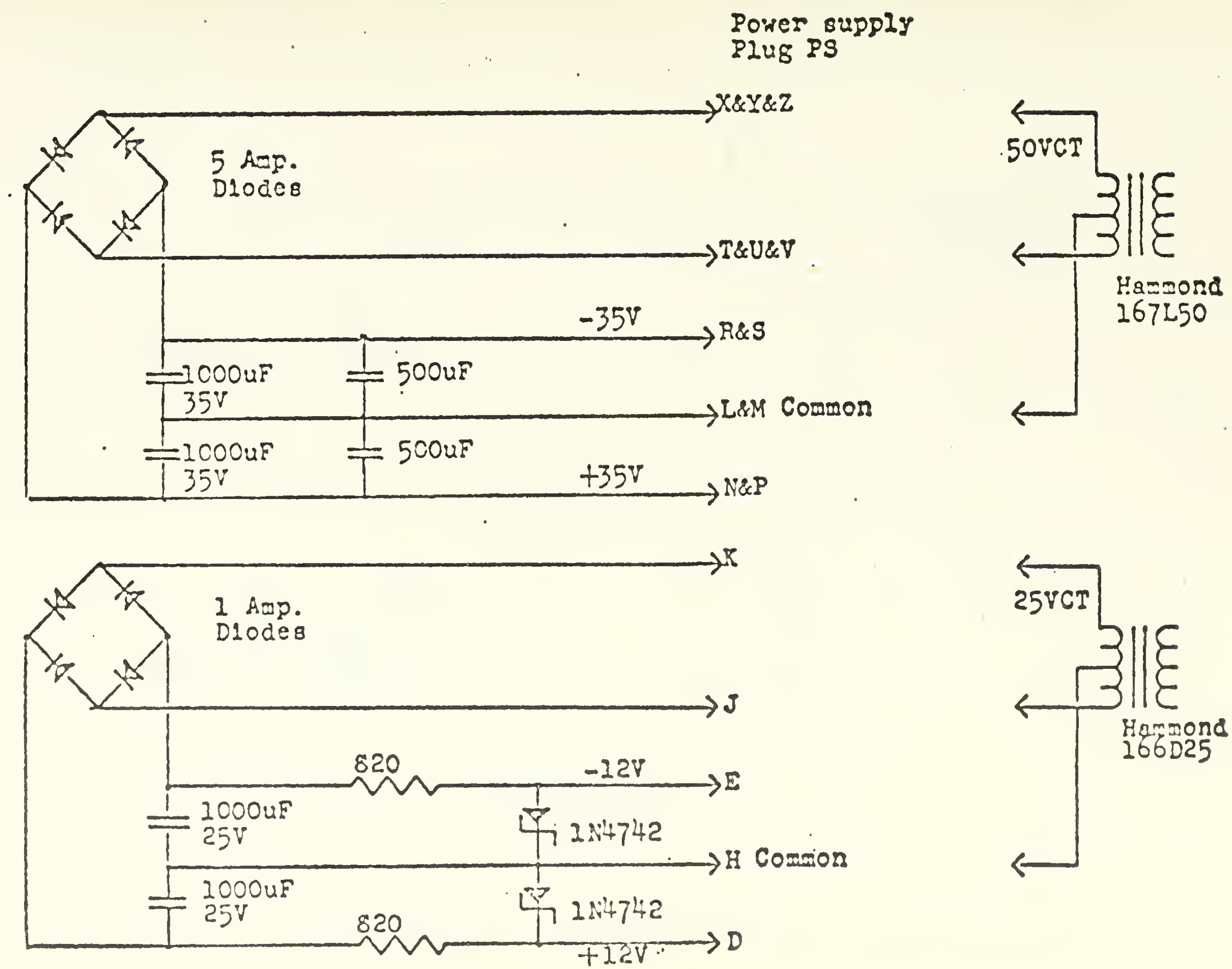

Figure 19. $\pm$ 35 and $\pm$ 12 Volt Power Supplies

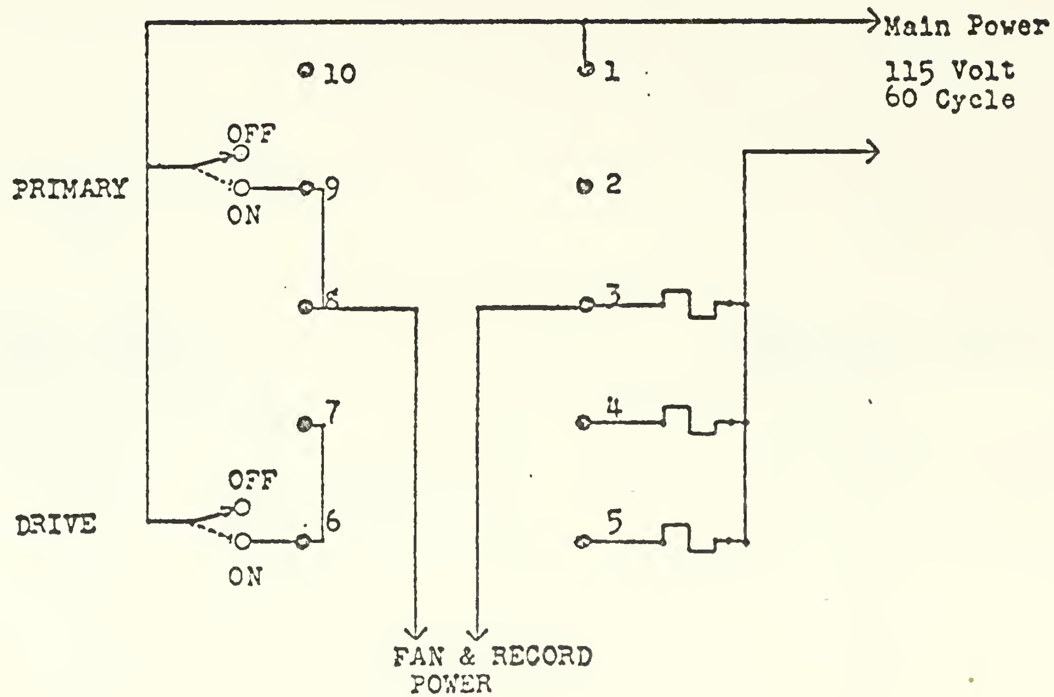

Figure 20. Wiring Diagram, AC Distribution to Power Supplies

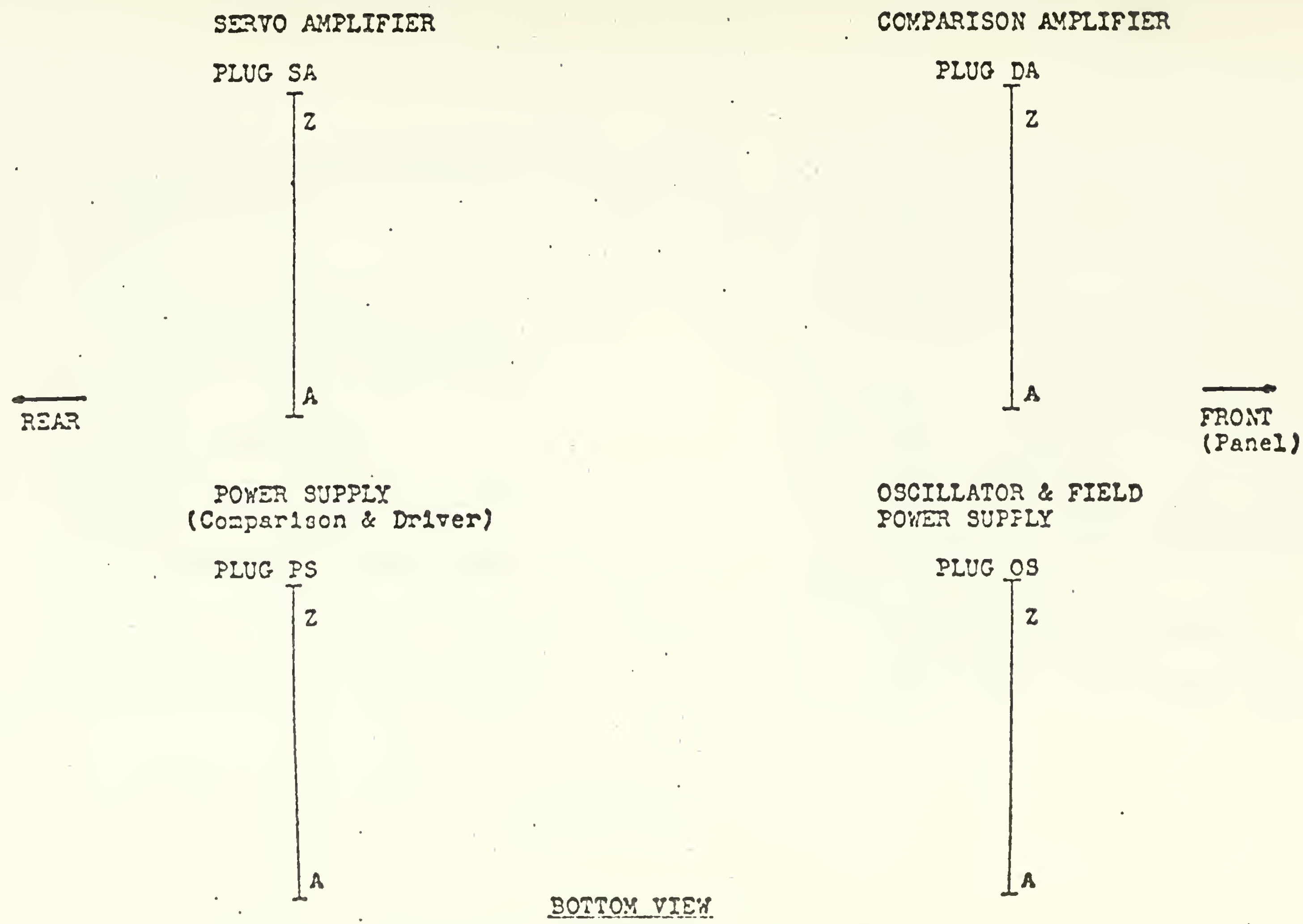

Figure 21. Chassis Mounted Circuit Board Placement

PLUG SA

PIN	
Z	Plus 35 Volts from PS(N,P).
Y	NC
X	Common Ground.
W	NC
V	NC
U	NC
T	Feedback from Driver Output.
S	NC
R	Minus 35 Volts from PS(R,S).
P	NC
N	NC
M	Input from DA(M).
L	NC
K	Spare
J	NC
H	NC
F	To base of NPN Driver 2N3714.
E	NC
D	NC
C	Spare.
B	To base of PNP Driver 2N3790.
A	Common Ground.

PLUG DA

PIN	
Z	Input from REF. ADJ. (Panel).
Y	Common Ground.
X	NC
W	Input from ERROR ADJ. (Panel).
V	To DA(M).
U	Internal Connection
T	" "
S	" "
R	Minus 12 Volts from PS(E).
P	NC
N	Offset, not used.
M	Output to SA(M).
L	Plus 12 Volts from PS(D).
K	Offset, not used.
J	Plus signal to REF. ADJ. (Panel).
H	From REF. OUT Transformer.
F	" " " "
E	Common Ground
D	From ERROR OUT Transformer.
C	" " " "
B	Plus signal to ERROR ADJ. (Panel).
A	Spare.

BOTTOM VIEW

Figure 22. Circuit Board Connector Wiring for Plugs SA and DA

PLUG PS

PIN	
Z	50 Volts AC Transformer 167L50.
Y	" " " " "
X	" " " " "
W	NC
V	50 Volts AC Transformer 167L50.
U	" " " " "
T	" " " " "
S	Minus 35 Volts to Driver & SA(R).
R	" " " " "
P	Plus 35 Volts to Driver & SA(Z).
N	" " " " "
M	0 Volts Common Ground.
L	" " " "
K	25 Volts AC Transformer 166D25.
J	25 Volts AC Transformer 166D25.
H	0 Volts Common Ground.
F	NC
E	Minus 12 Volts to DA(R).
D	Plus 12 Volts to DA(L).
C	Spare.
B	Spare.
A	Spare.

PLUG OS

PIN	
Z	One leg each Osc. Out Transformer.
Y	NC
X	Pri. Osc. Out Ref. Transformer.
W	NC
V	Pri. Osc. Out Error Transformer.
U	NC
T	Internal Minus 24 Volts to meter.
S	NC
R	Internal connection.
P	" "
N	Common Ground.
M	Internal connection.
L	" "
K	1500 Ohms from H for Alarm Plus.
J	NC
H	Plus 28 Volts to Motor Field.
F	NC
E	Minus 28 Volts to Common Ground.
D	NC
C	25 Volts AC Transformer 166J25.
B	NC
A	25 Volts AC Transformer 166J25.

BOTTOM VIEW

Figure 23. Circuit Board Connector Wiring for Plugs PS and OS

OSC./REF. TRANSFORMER PRI.	1	24 VOLTS METER 24 VOLT OSC. PWR.
	2	NC
SWITCH & RAISE/LOWER POT.	3	ERROR TRANSFORMER SEC. PROBE TRANSFORMER SEC.
OSC./ERROR TRANSFORMER PRI.	4	ERROR OUTPUT BLUE TRANSFORMER PRI.
SWITCH & RAISE/LOWER POT.	5	ERROR OUTPUT RED PRI. PROBE TRANSFORMER SEC.
	6	NC
OSC./REF. TRANSFORMER SEC.	7	REF. OUTPUT TRANSFORMER PRI. BLUE
OSC./REF. TRANSFORMER SEC.	8	REF. BAL. POT.
	9	REF. BAL. POT. REF. OUTPUT PRI. RED
	10	NC

ARMATURE (GND.)	#3 Pin
ARMATURE (HI)	#6 Pin
FIELD (GND.)	#4 Pin
FIELD (HI)	#5 Pin
TACHOMETER	#2 Pin
TACHOMETER	#1 Pin

DRIVE MOTOR CHASSIS AND CABLE CONNECTION DETAIL

POT. SLIDER (GREEN)	A Pin
LOW END POT (BLK)	B Pin
PROBE	C Pin
PROBE	D Pin
SPARE (BROWN)	E Pin
HIGH END POT (RED)	F Pin
ALARM	G Pin

Figure 24. Distribution Terminal Strip (Under Chassis) for Oscillator and Reference/Error Circuits

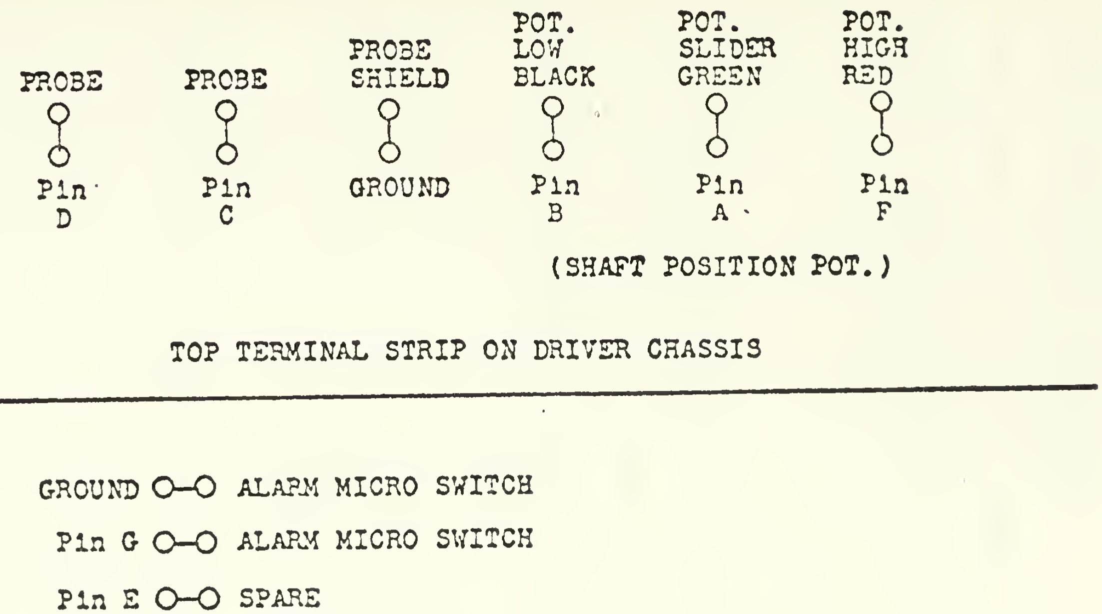

Figure 25. Lower Terminal Strip on Driver Chassis

Other information is contained in the designer's unpublished specification and operation manual.

E. OCEAN CONFIGURATION

1. Spar Buoy/Wind Vane Design

In the spar buoy/wind vane design, the instrument is mounted in an electronics compartment inside a wind vane which in turn is mounted on a spar buoy. The wind vane and spar buoy configuration is shown in figures 26 and 27.

The wind vane and electronics compartment are manufactured from heavy aluminum stock. A stainless steel cowling, hinged at the pointed end for easy equipment access, provides wave and weather protection. A junction panel located at the top of the wind vane has six coaxial feed-through connectors. The cable linking head to output assembly is also connected at this point. Weight of the wind vane with electronics installed is 87kg (190 pounds).

The spar buoy is designed to carry the wind vane approximately 60 cm (2 feet) above the water surface. It is constructed of No. 16 gauge galvanized steel with one-quarter inch steel end plates. A one inch steel pipe is positioned in the center of the spar and welded to the end plates. The buoy is filled with hand-mixed styrofoam. It displaces approximately 400 pounds fully submerged and has a natural period of oscillation of approximately three seconds. A steel slot on top of the buoy is used to secure the wind vane.

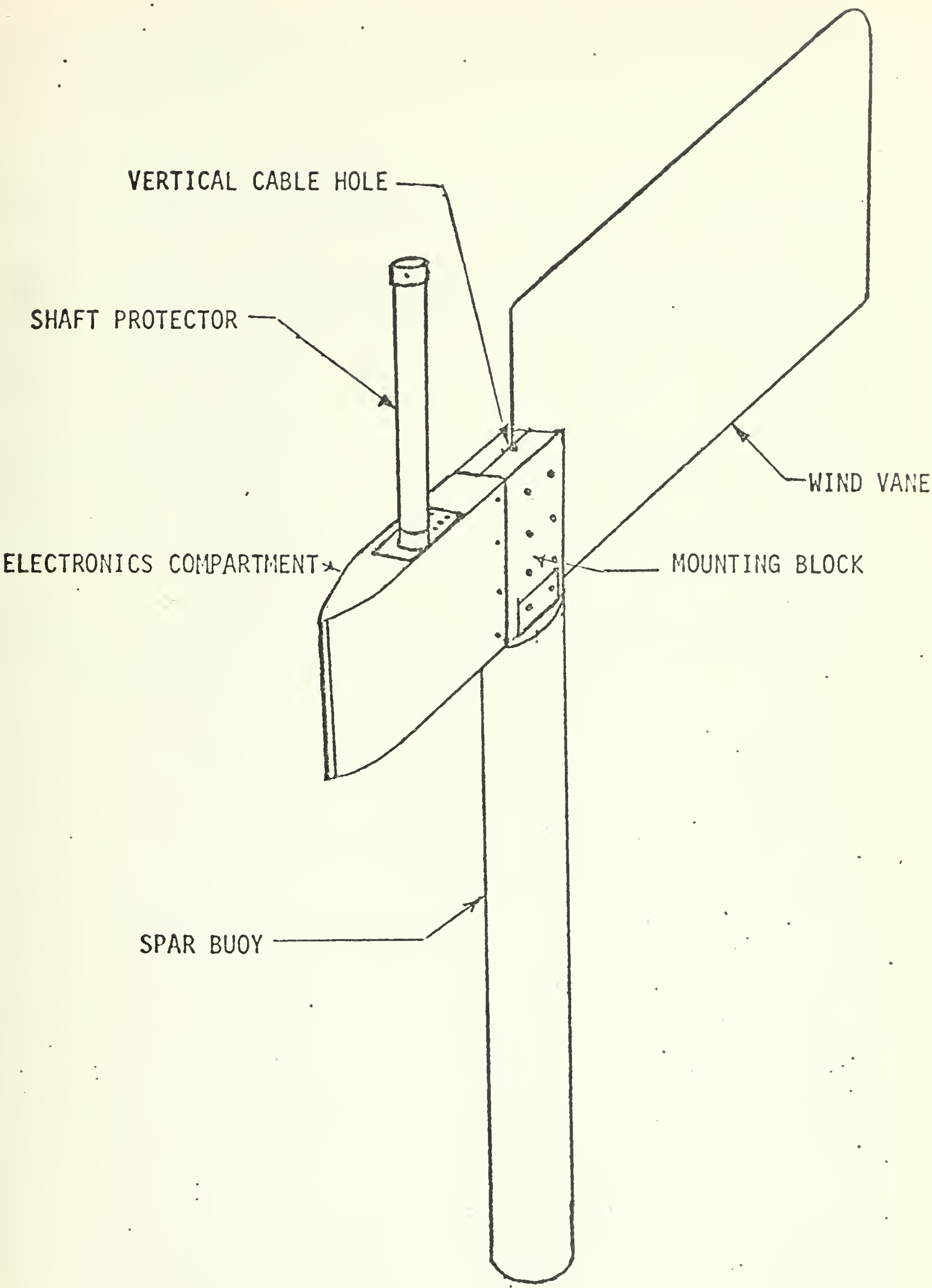

Figure 26. Nomenclature for Spar Buoy/Wind Vane Configuration Perspective View

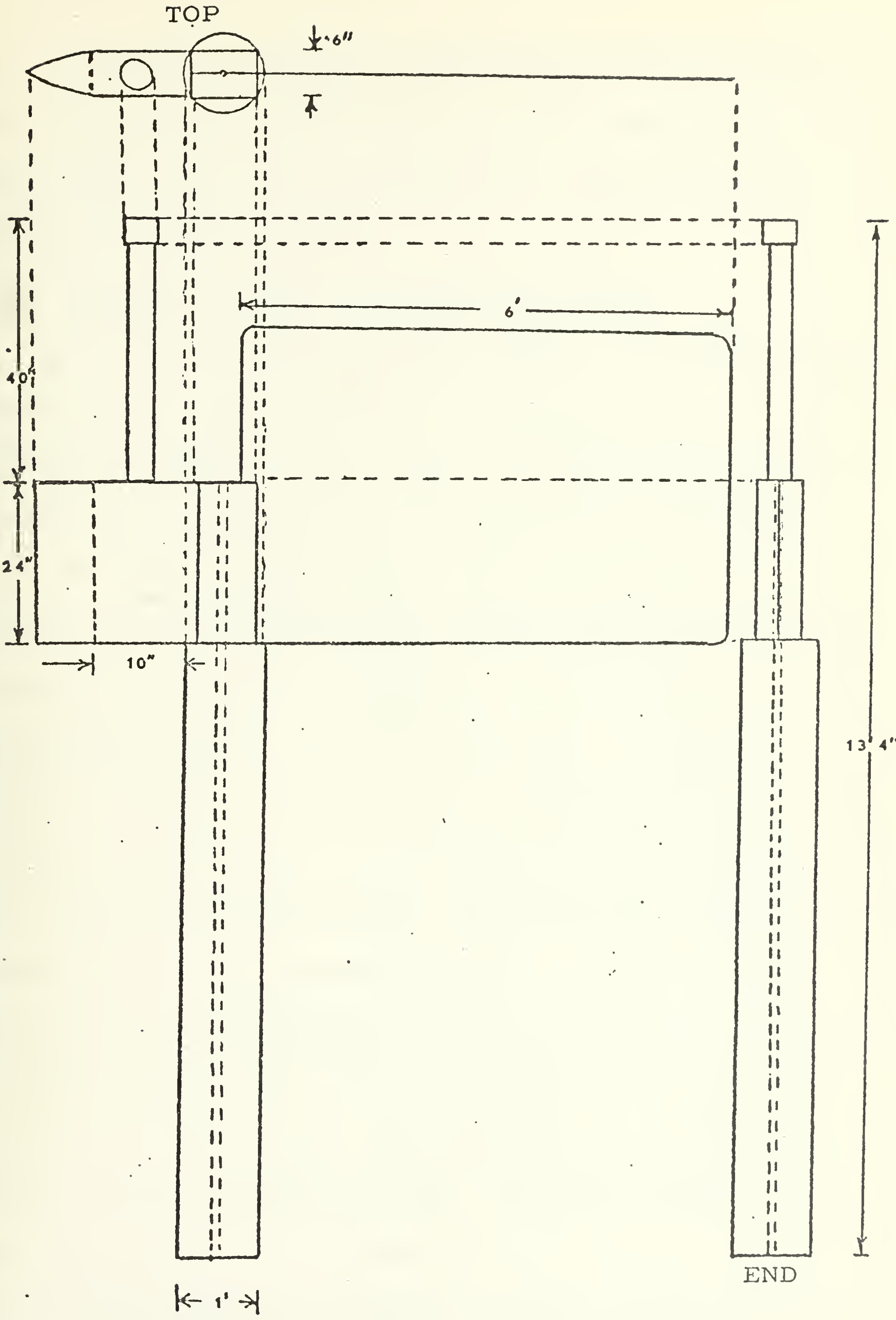

Figure 27. Spar Buoy/Wind Vane Configuration.
Top, Front, and Side Views

In operation, the buoy and vane slide up and down on a taut vertical cable. The buoy follows the wave profile of the low frequency high amplitude waves while the electronic sensor follows the smaller amplitude, high frequency waves.

2. Catamaran/Neutral Buoyancy Cylinder Design

The catamaran/neutral buoyancy cylinder was designed to overcome deficiencies in the spar buoy/wind vane configuration. The system is tethered to a supporting vessel and positioned sufficiently far away so as to operate in a relatively undisturbed wind and wave environment.

The buoy consists of a large wind vane, supporting A-frame, catamaran pontoons, neutral buoyancy cylinder, and a weighted righting arm (figure 28). Frame and connecting structure were made of 1 inch galvanized steel conduit welded and bolted together. The pontoons are made of 8 inch thin walled aluminum pipe, sealed and angled at each end. The neutral buoyancy cylinder was fabricated from 1/16 in stainless steel sheet. It is filled with styrofoam and sealed at both ends with light weight steel end plates. A steel pipe runs through the cylinder to house and secure one end of the righting arm. Its large cross sectional area serves as a damping plate to reduce heave. The righting arm is made of a 20 foot section of 3 inch diameter, thick-walled pvc pipe. Plastic sleeves at either end provide additional strength. Four donut shaped 50 pound lead weights are pinned to the terminal end of the pvc pipe. Since the neutral buoyancy cylinder was designed to displace all but 20 pounds of

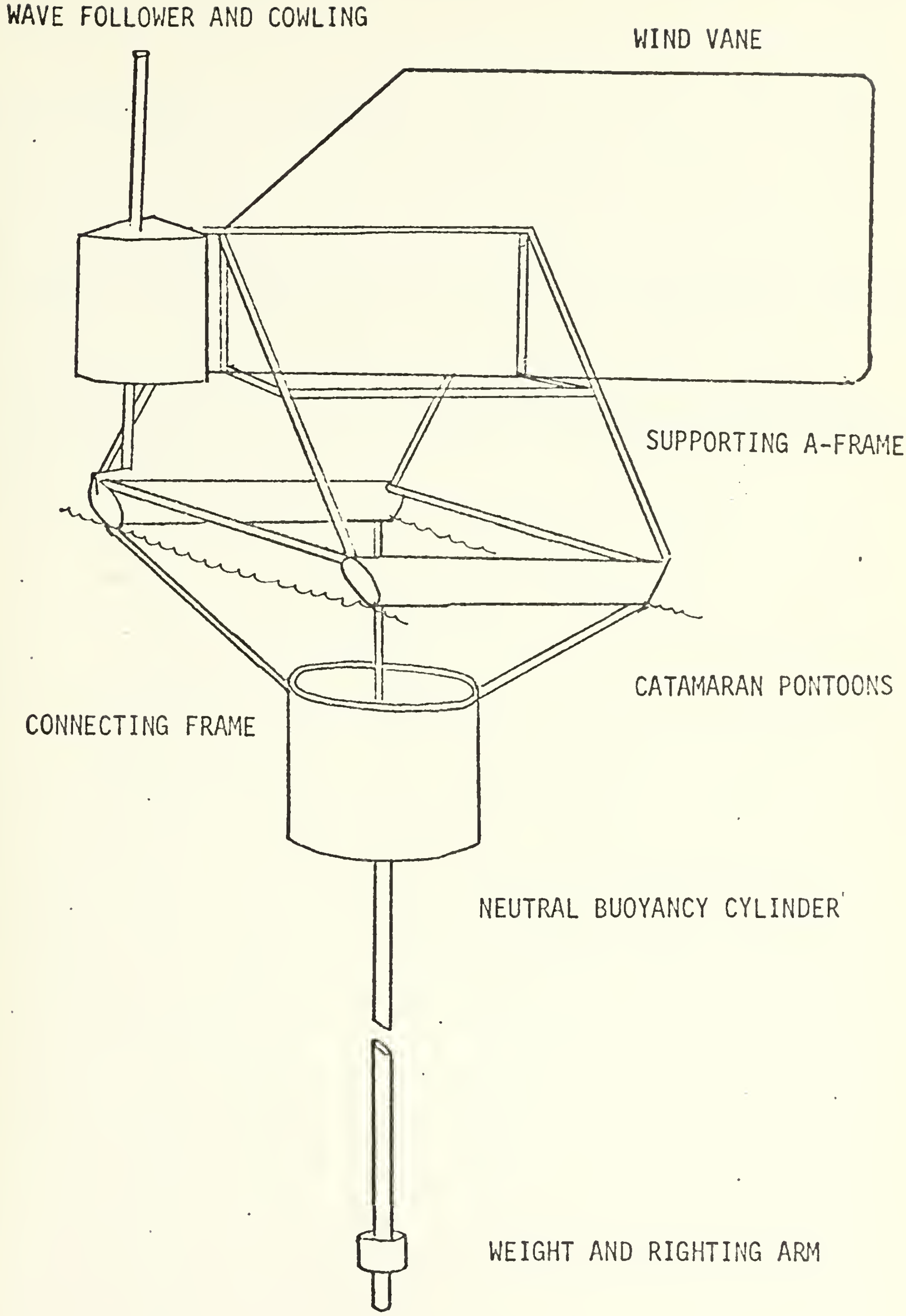

Figure 28. Nomenclature for Catamaran and Neutral Buoyancy Cylinder Configuration, Perspective View

the structure's total weight, the system sinks to and floats on the catamaran pontoons. The wind vane is made of 3/8 inch plywood suitably treated for the marine environment. The wave follower and cowling assembly are designed so that they can be easily attached or removed while the buoy is already in the water. Dimensions for the buoy are shown in figure 29. Consideration was given to balancing and stabilizing the buoy so that the center of gravity would lie along the righting arm axis. Much of the design takes advantage of materials and manufacturing techniques readily available.

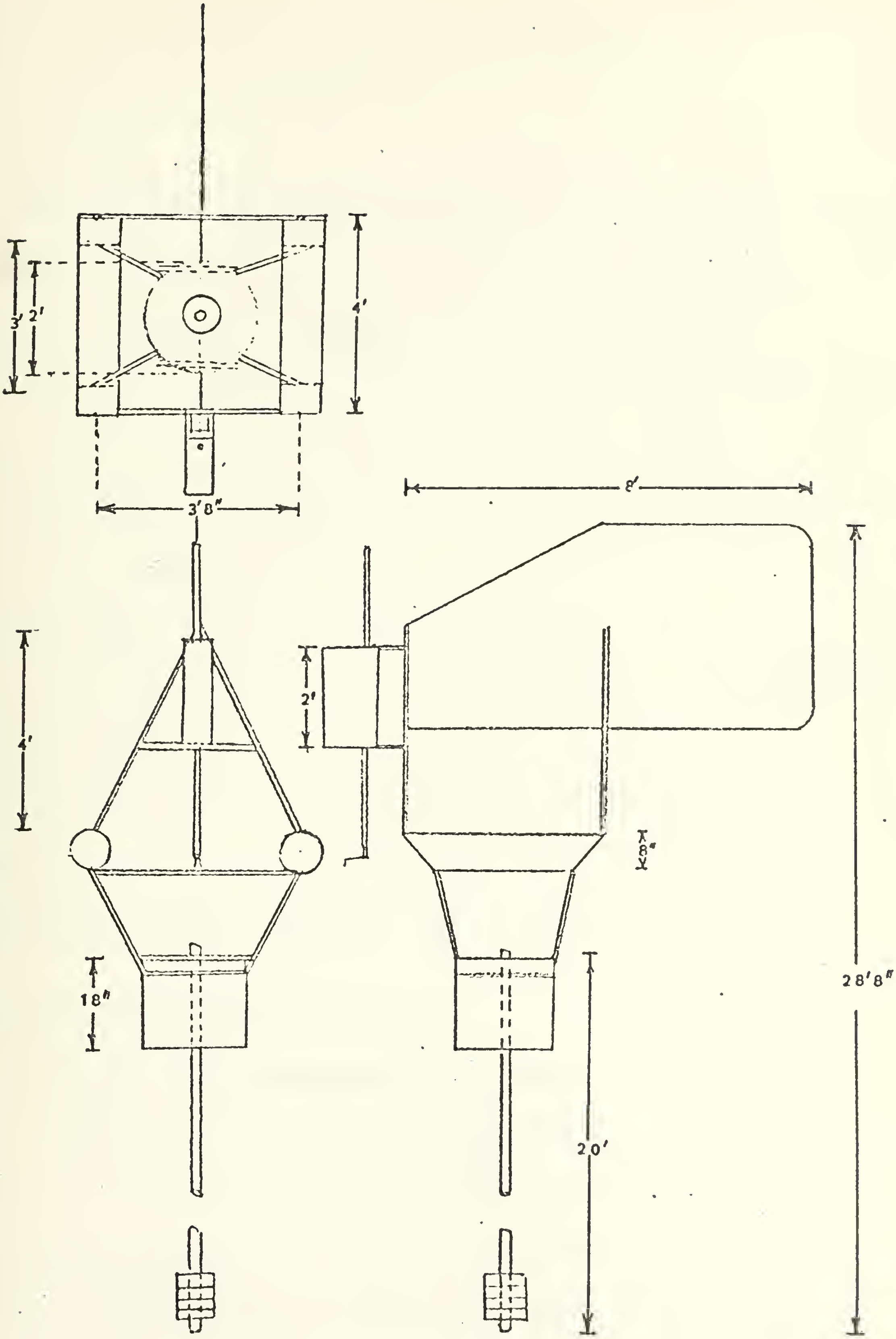

Figure 29. Catamaran/Neutral Buoyancy Cylinder Configuration. Top, Front and Side Views

IV. TESTS AND EVALUATION

A. GENERAL

The tests and evaluation of the LOWFER were designed to determine system operating characteristics in both the laboratory and field. The purpose of the experiments was two-fold: (1) to determine the instrument's ability to accurately follow a given shaped wave at various amplitudes and frequencies and (2) to determine the wave follower's response to a broad frequency band wave regime. Other laboratory experiments included the observation of wave follower characteristics when subjected to shaft loading, when tilted relative to the water surface, and when probe sensor wires were placed in various configurations. Field experiments included taking measurements to ascertain the wave follower response characteristics in near shore and in open sea conditions. In addition, field observations of the spar buoy and catamaran systems were made and methods for their deployment were developed.

B. LABORATORY EXPERIMENTS

1. Narrow Frequency Band Experiment

The narrow frequency band experiment was conducted in a long narrow wave tank utilizing a paddle driven wave generator capable of producing nearly sinusoidal waves of 0-3 Hz and up to 20 cm in wave height. Measurements were taken at a distance 10 m from the wave

generator paddle assembly. Because of shoaling properties of the wave tank (a result of continuously decreasing water depth along the wave tank's length), the originally produced waves were altered to a non-sinusoidal shape. At the opposite end, a perforated steel beach with spongy damping material substantially reduced wave reflections that might have interfered in the measurement area. Figure 30 shows the experimental setup along with the wave tank dimensions.

A miniature capacitance wave gage was secured to the shaft of the wave follower in the immediate vicinity of the wave sensor. Any change from the initial immersion point on the wave gage produced an error signal which was indicative of the way the instrument was tracking the wave profile. Improvement of wave follower sensitivity and accuracy could be made by carefully adjusting the Ref Adj. and Error Adj. to minimize the error signal. The signal was not used as an indication of true error however, as dragging of water by the wave gauge wire occurred as the shaft moved up and down. In a similar manner, a stationary mounted capacitance wave gage was used to measure the wave profile adjacent to the shaft probe sensor. The electronic circuit for the capacitance wave gages (figure 31) was adjusted so that it produced a linear voltage output as a function of wave height. The stationary wave gage was calibrated in still water using a digital voltmeter to monitor depth changes. Recorder settings were then adjusted to give desired deflections. Along with the wave gage outputs, signals from the shaft

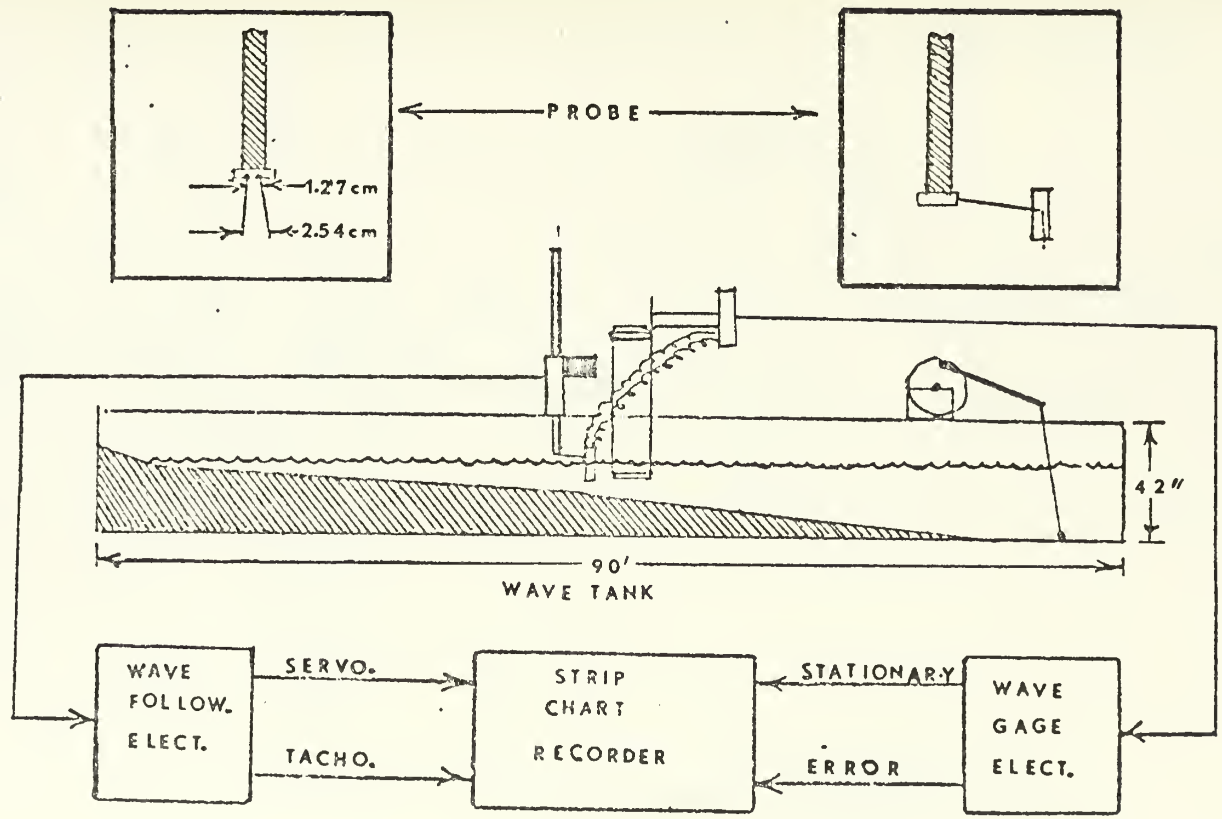

Figure 30. Block Diagram, Narrow Frequency Band Experiment

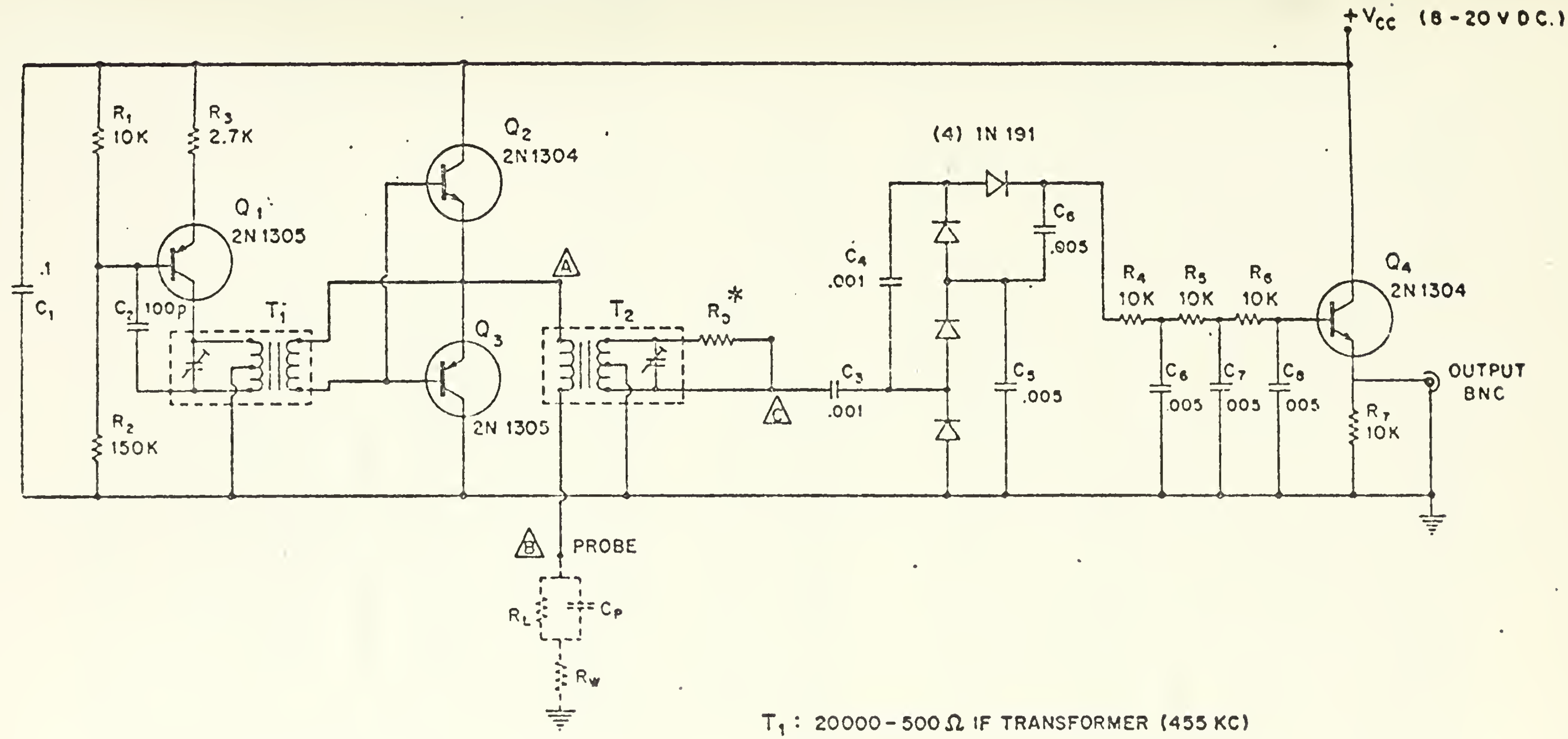

T_1 : 20000 - 500 Ω IF TRANSFORMER (455 KC)

T_2 : 50000 - 500 Ω IF TRANSFORMER (455 KC)

ALL CAPACITORS IN μf. UNLESS OTHERWISE NOTED

Figure 31. Capacitance Wave Gage Electronics
(After McGoldrick, 1969)

position potentiometer and from the tachometer circuit were monitored on a Brush 8-channel strip chart recorder.

In the first experiment, the wave follower was subjected to a wide range of wave conditions to determine how well the instrument could follow waves of different frequency, amplitude and steepness. Representative strip chart recordings are shown in figures 32, 33, and 34. Of particular significance is the faithful reproduction of the wave profile, the phase relationship between the shaft position and the stationary wave staff output, and to a lesser extent, the characteristic signal from the error wave staff. In each figure, percent-error has been calculated according to the relationship:

$$\frac{|\text{Stationary Wave Gage Height} - \text{Shaft Position Height}|}{\text{Stationary Wave Gage Height}} \times 100 = \text{Percent-Error}$$

Height in all cases refers to the peak to peak (crest to trough) signal amplitude. In each figure (figures 32, 33, 34) the arrow indicates the point of measurement. Percent-error was greatly influenced by the wave height to wavelength ratio and by the degree of pointedness of the wave crest. In figure 33, the expected damped oscillation wave form indicative of servo hunting is clearly illustrated. Because the shaft position is smooth and very similar to the stationary wave staff signal, it is seen that the degree of hunting is relatively small. In the figures shown and in all other cases where valid tests were made, percent-error is 7% or less.

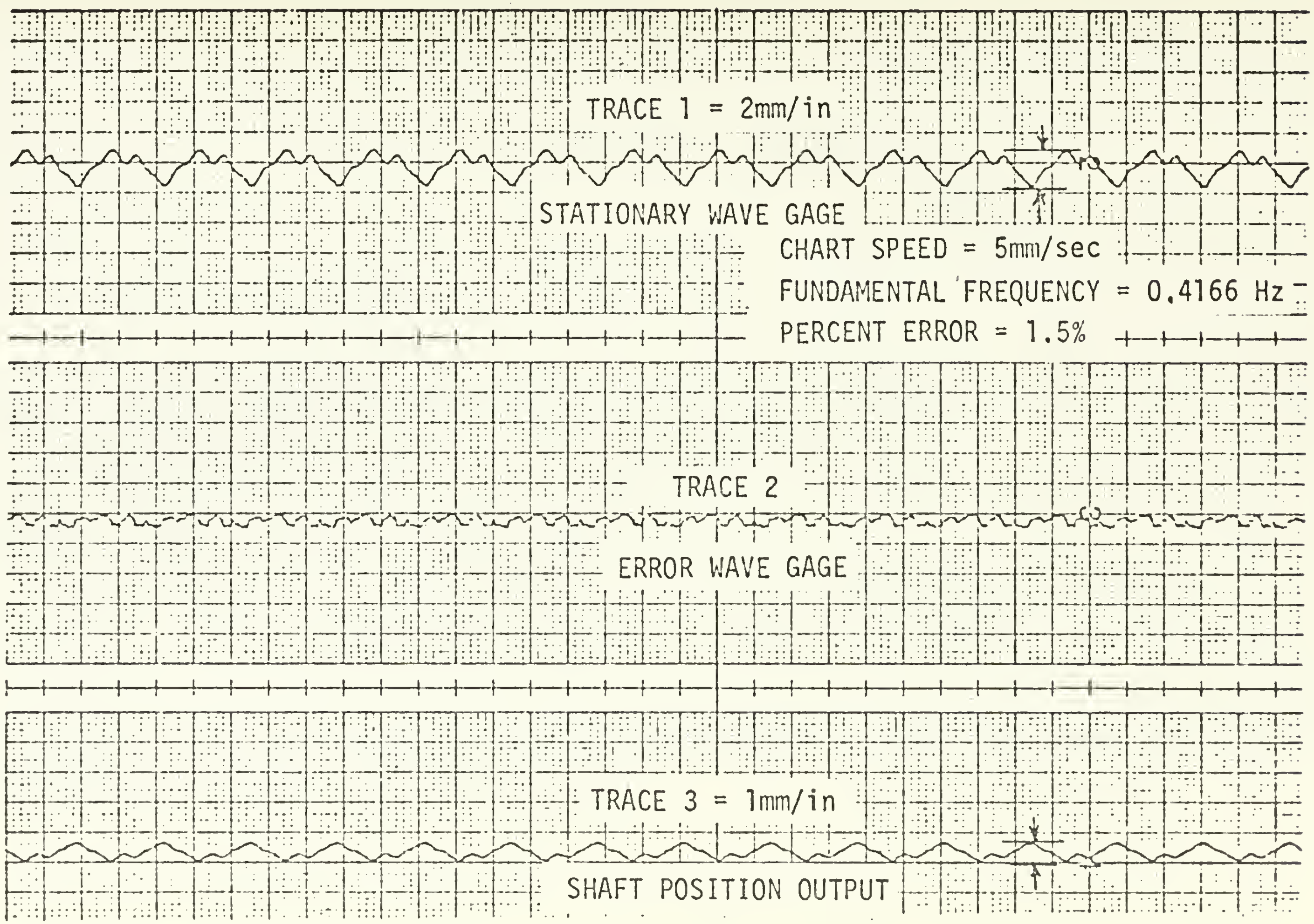

Figure 32. Narrow Frequency Band, Low Fundamental Frequency

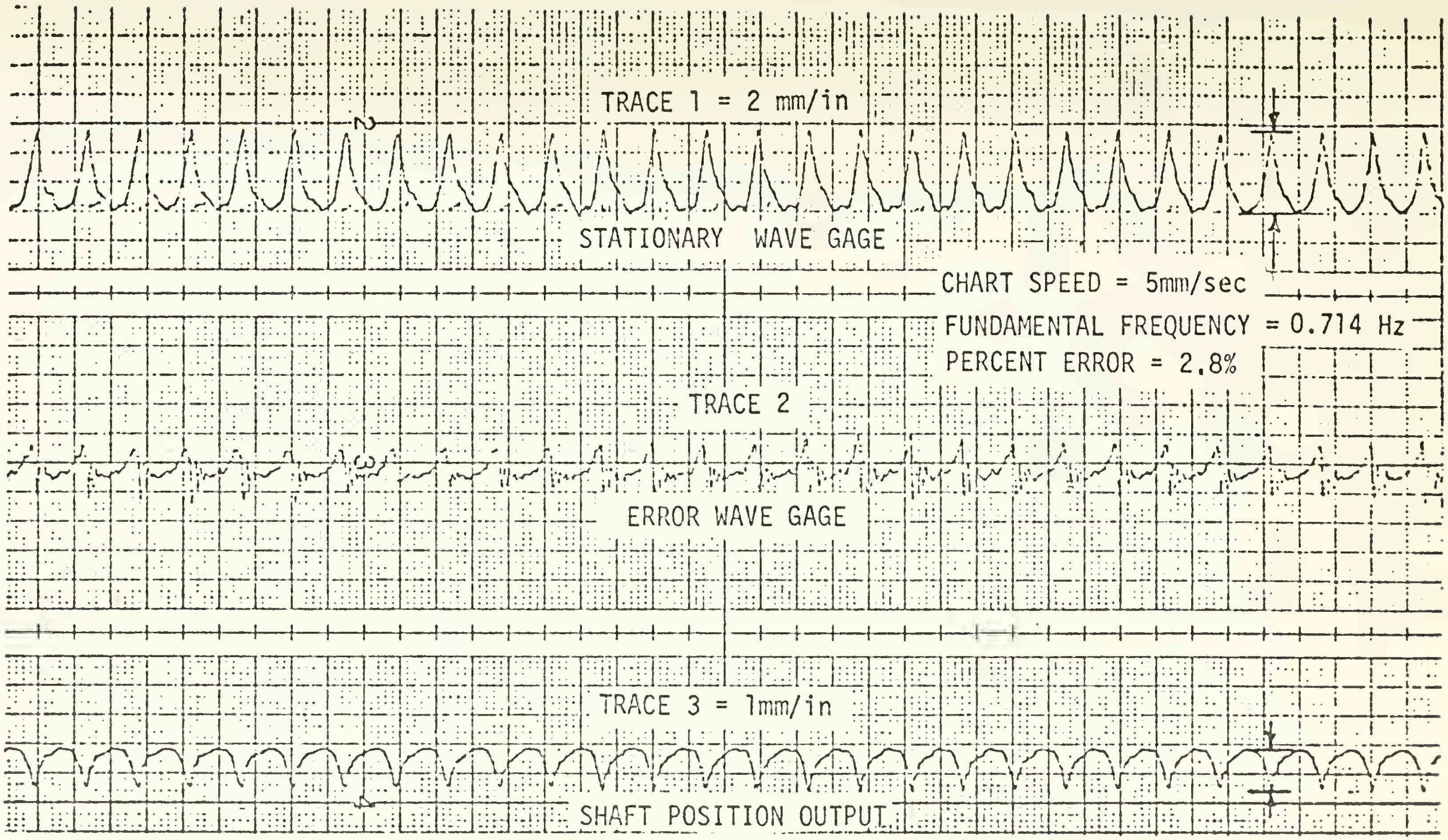

Figure 33. Narrow Frequency Band, Medium Fundamental Frequency

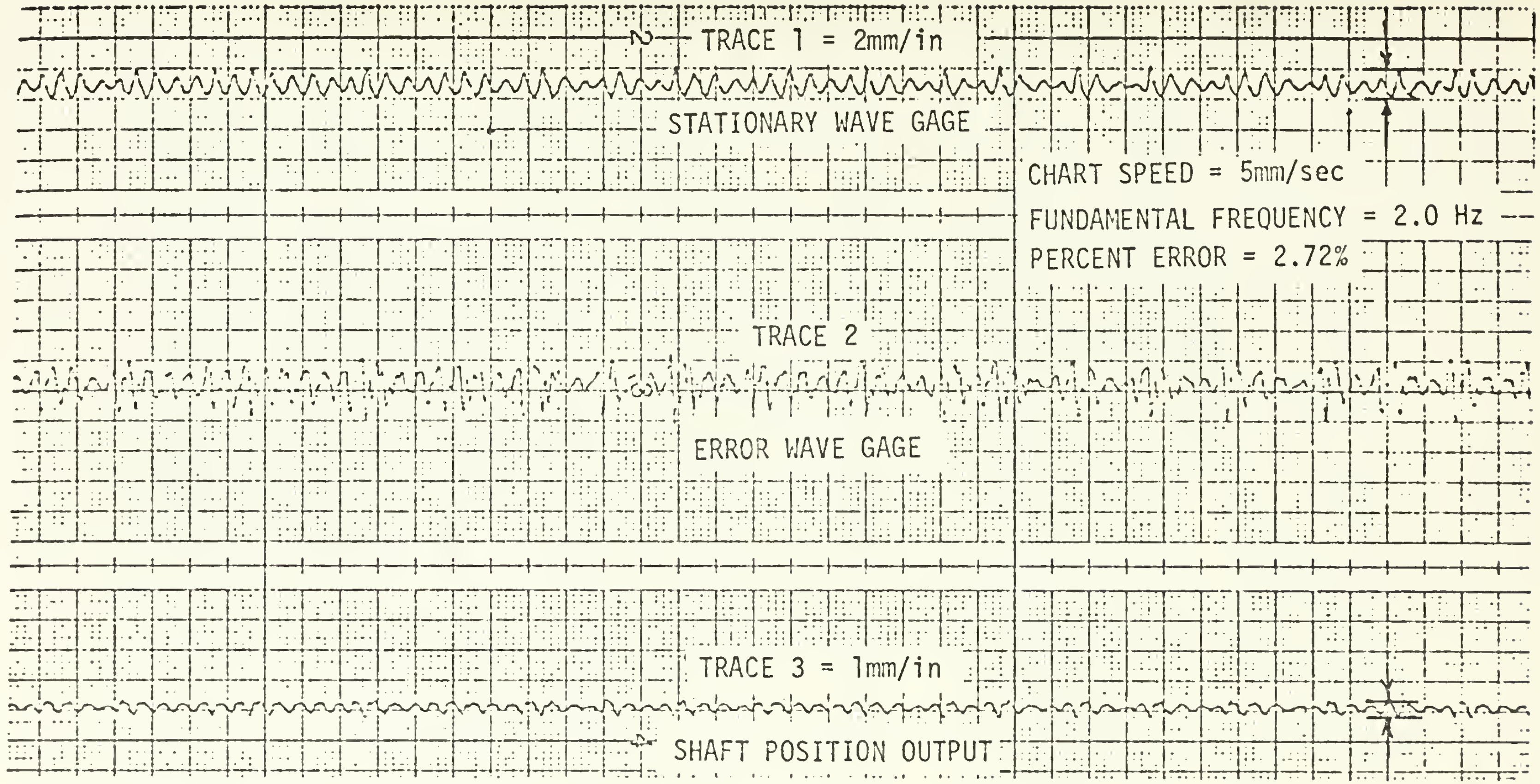

Figure 34. Narrow Frequency Band, High Fundamental Frequency

A similar series of experiments was conducted with a 0.5 kg weight securely attached to the shaft to simulate an array of sensors. Results indicate little degradation of equipment performance (figures 35 and 36). It was noted, however, that spurious shaft position output signals often occurred as a result of excessive shaft vibration when the load was concentrated in a small area.

In another experiment, the wave follower was tilted 20 degrees from the vertical in the vertical axis/transverse axis plane of the wave tank. Signal outputs indicate only slight differences between the tilted and untilted condition (figure 37).

In all experiments, the tachometer circuit output null point (zero voltage) occurs at a turnaround point of the shaft movement (the lowest point of a wave trough or highest point of a wave crest). In spite of the erratic appearance of the tachometer signal, the net effect is to amplify small perturbations of shaft movement which may prove useful in future studies (figure 38).

All tests conducted during this experiment were done so with a probe sensor spacing of 1.28 cm at the shaft end and 2.54 cm at the water end (Insert, figure 30). It was found that the system was sensitive to wire spacing but that a wide variety of spacings produced similar results. Therefore, for standardization, the aforementioned sensor wire spacing was maintained.

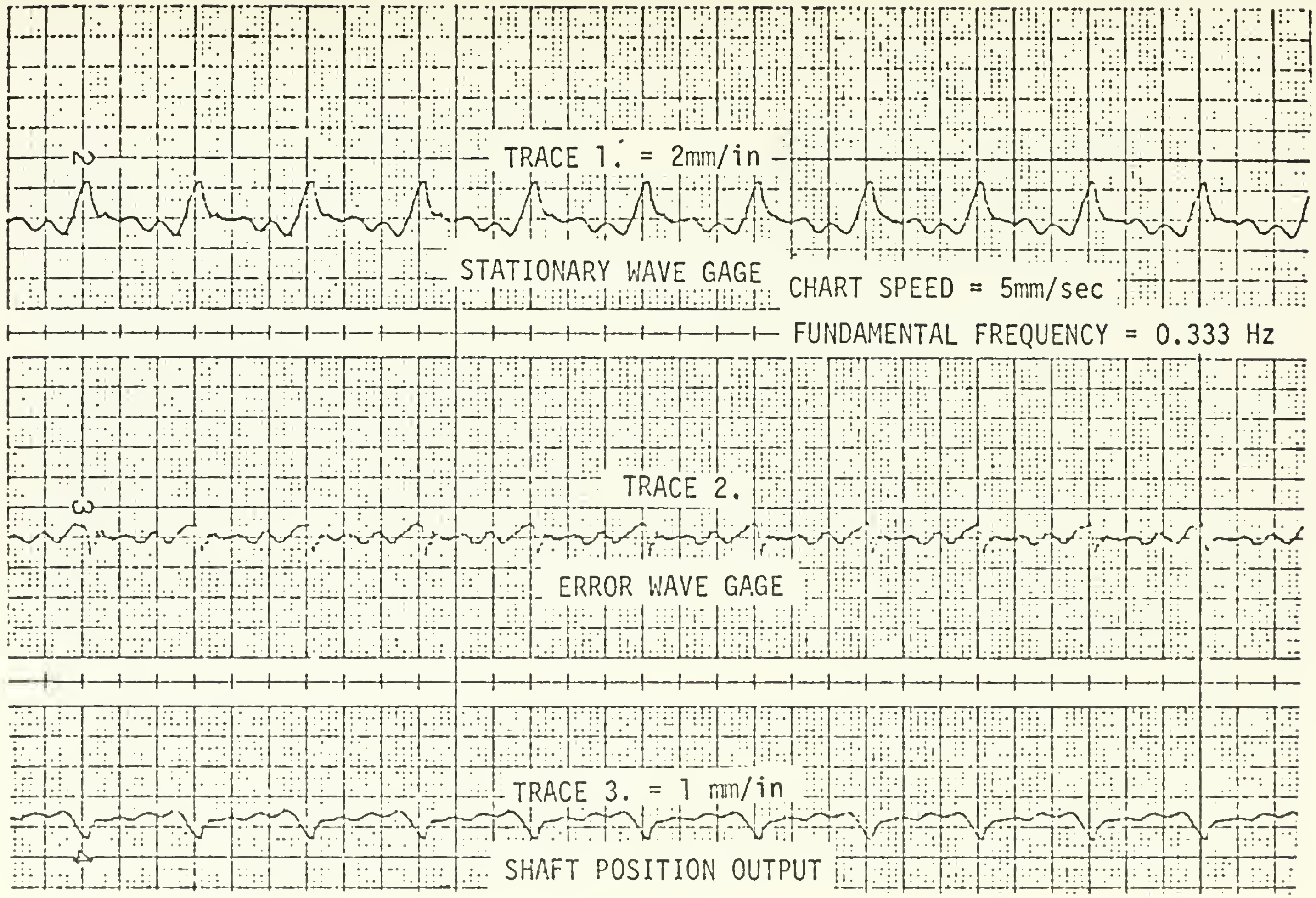

Figure 35. Low Frequency, 0.5 kg Weight Attached to Shaft

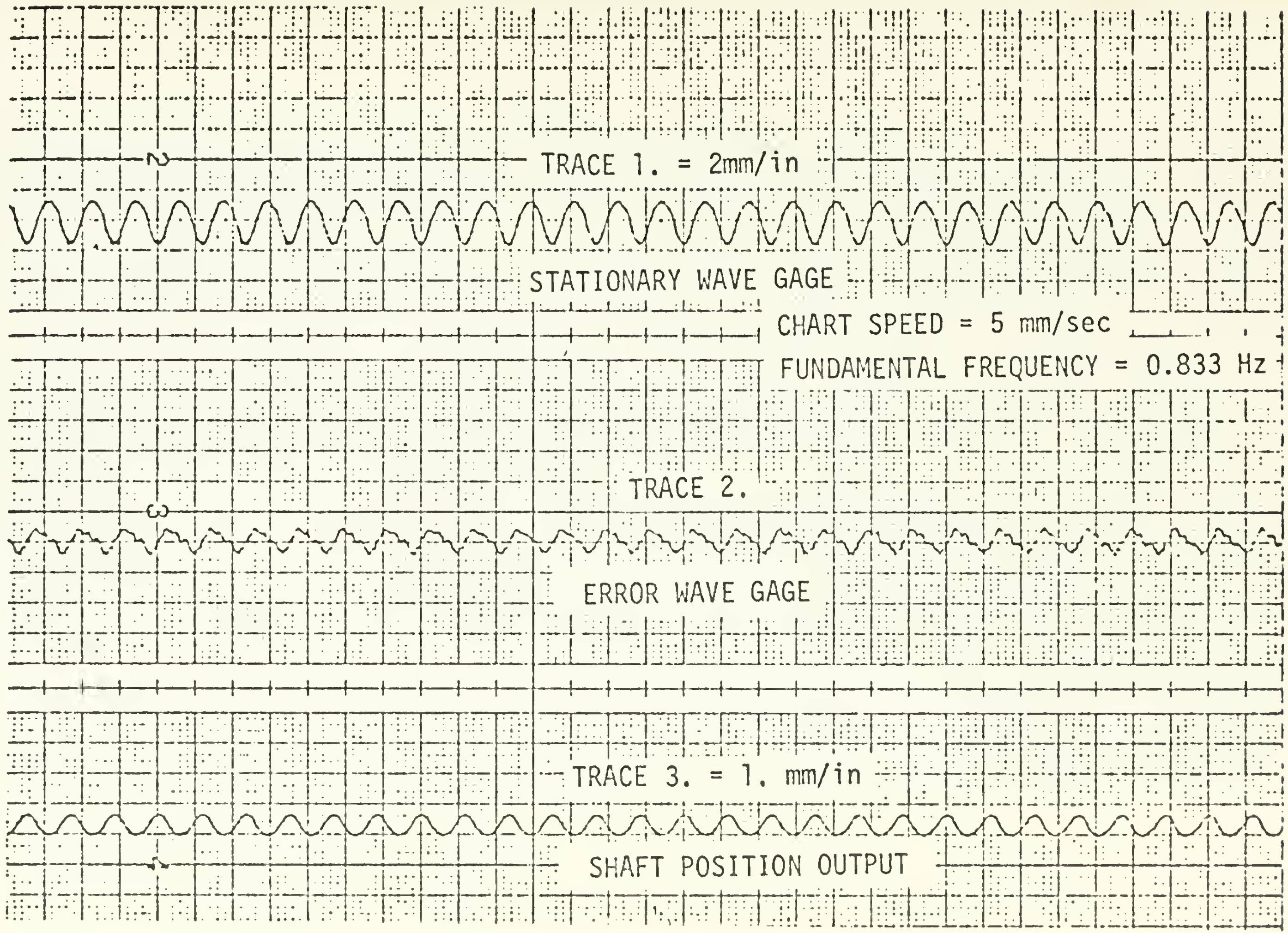

Figure 36. Medium Frequency, 0.5 kg Weight Attached to Shaft

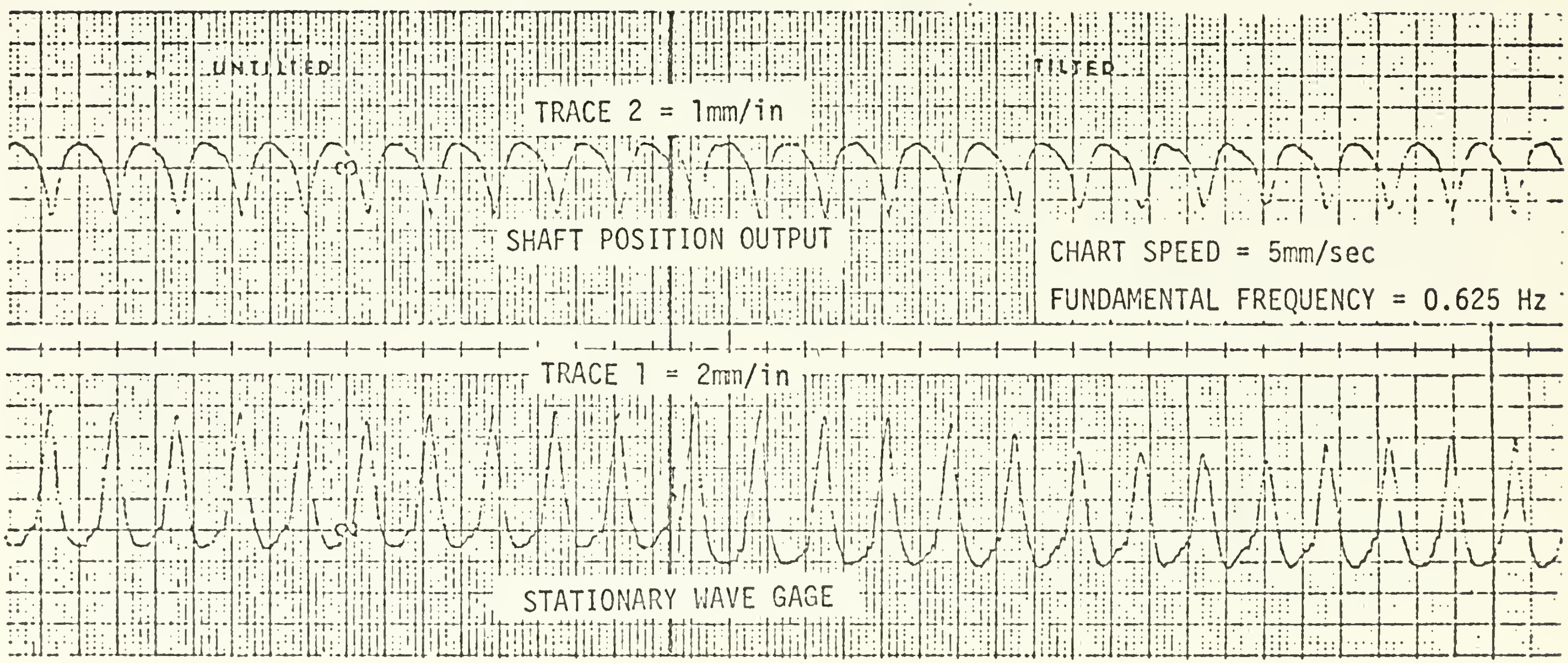

Figure 37. Wave Follower Tilted 20° to Vertical

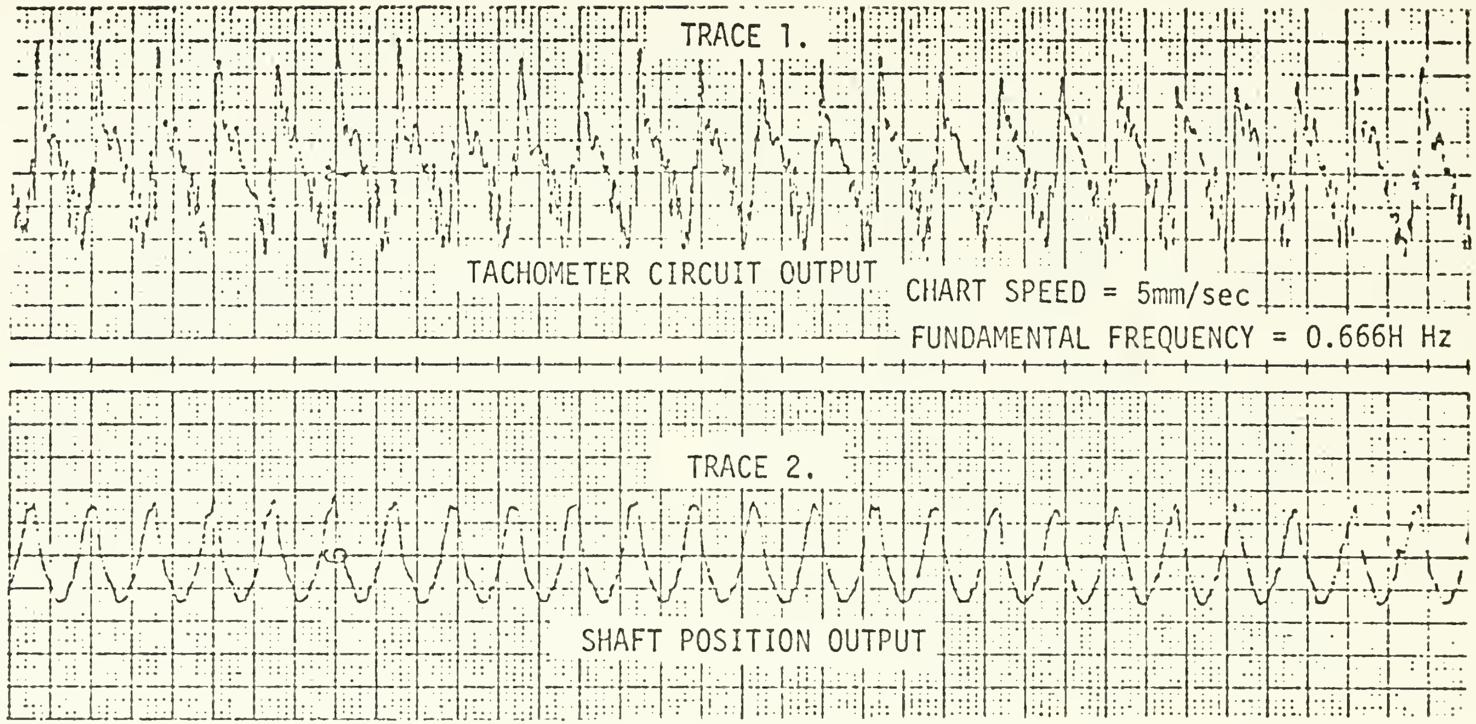

Figure 38. Tachometer Circuit Output

2. Broad Frequency Band Experiment

The wind-generated wave experiment was conducted to determine the wave follower characteristics in a controlled multi-frequency wave environment. Tests were conducted in a manner similar to those in the narrow frequency band experiment but also included additional data collection utilizing a Sanborn 14 channel electro-magnetic tape recorder. In addition, the output signals from the shaft position potentiometer and from the stationary wave gage were low pass filtered (0-20 Hz) with two Kron-hite Model 3540P active filters to eliminate possible 60 Hz interference (figure 39). During the experiment, system adjustments for best accuracy were made primarily by eye, as the wave regime was exceedingly complicated and could not be done using strip chart output signals.

Different wave regimes were set up using two, three or five wind generating fans respectively. Ten minutes of data for each regime were recorded. Raw voltage data from the Sanborn 14 channel tape recorder were digitized at one-msec intervals by a Vidar analog to digital tape recorder. The digitized files were then processed with the IBM 360/67 computer utilizing a program that provides options for calculating auto-correlation, power spectra, coherence, and phase (figure 40). By stipulating various program parameters, a Nyquist frequency of 15.6 Hz was imposed. Plots of power spectra for shaft position and stationary wave gage output coherence between the two

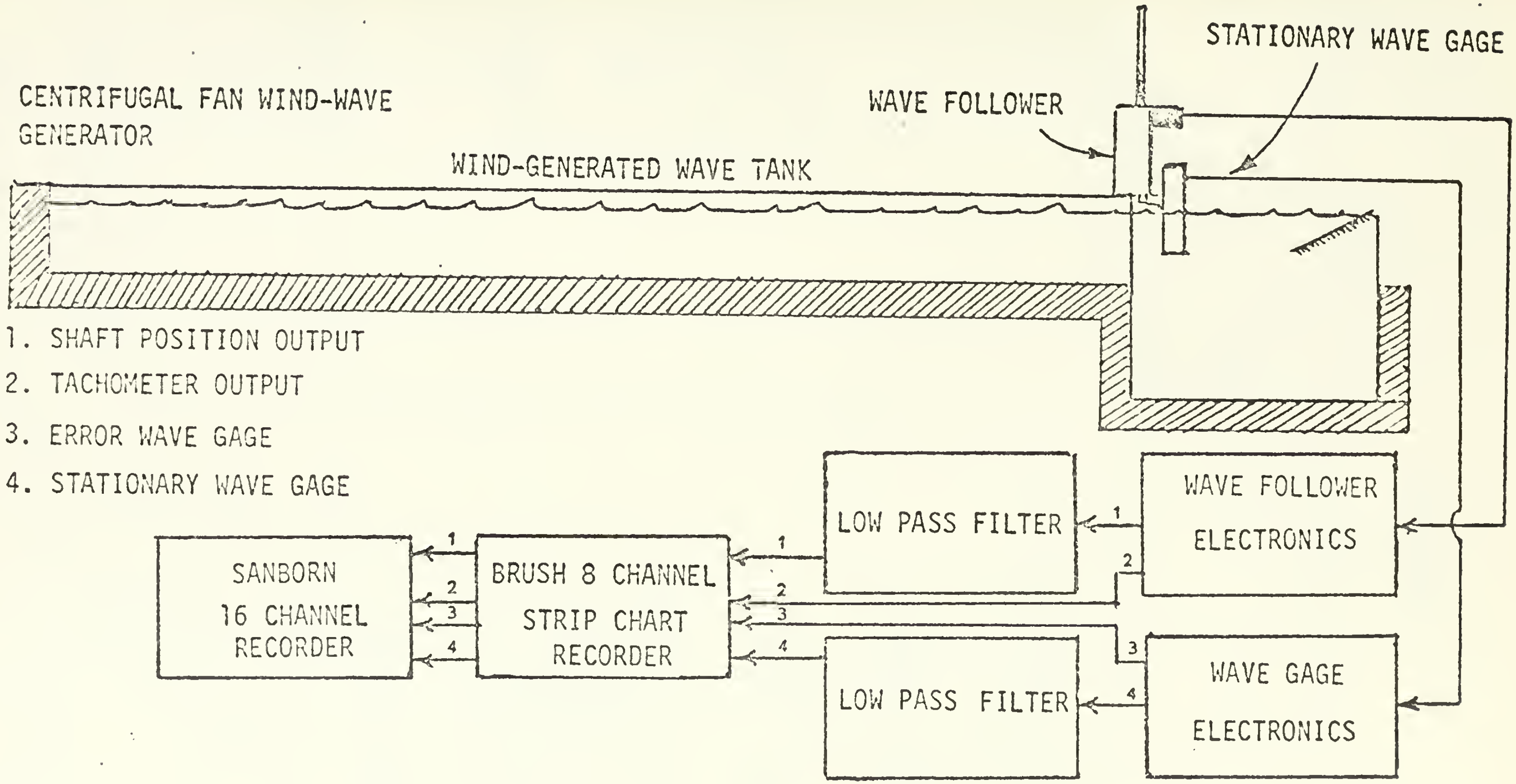

Figure 39. Block Diagram, Broad Frequency Band Experiment

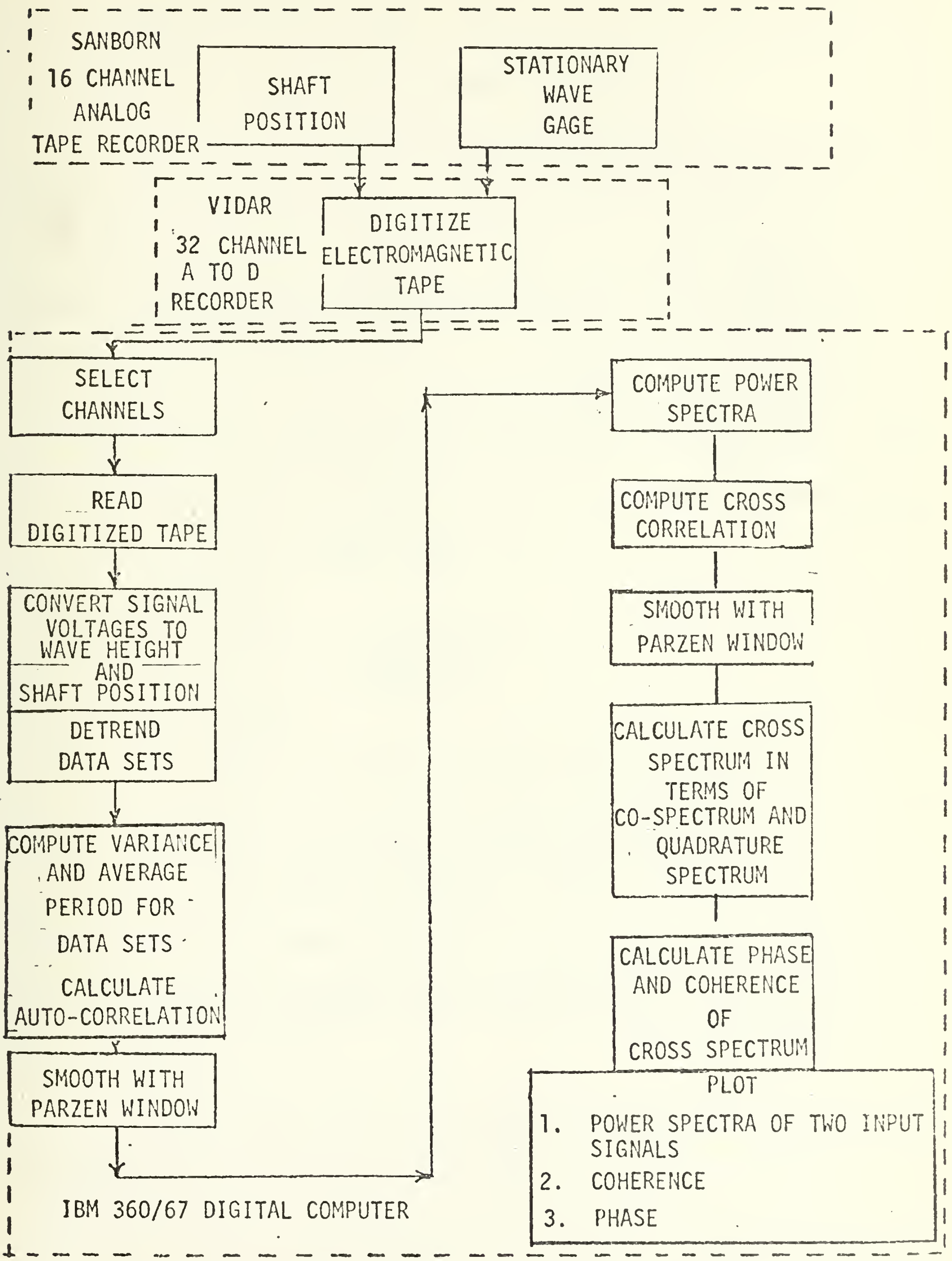

Figure 40. Data Collection and Analysis Flow Chart

signals, and their phase relationship for the different wave regimes are shown in figures 41, 42, and 43. In each case, close agreement is realized at frequencies where sufficient energies exist.

Since it is seen that the frequency spectrum in the wave follower output (shaft position signal) is similar to the frequency spectrum in the input (stationary wave staff spectrum) and because the amplitude and phase of the input frequency components appear to be independently modified by the wave follower, it is concluded that the wave follower is essentially a linear system over the frequency range of interest. Therefore, a linear transfer function can be calculated using the relationships:

$$S_y(f) = /H(f)/^2 S_x(f)$$

then

$$/H(f)/ = \left\{ \frac{S_y(f)}{S_x(f)} \right\}^{\frac{1}{2}}$$

where

$S_y(f)$ is the output energy spectrum value

$S_x(f)$ is the input energy spectrum value

and $/H(f)/$ is the linear transfer function.

Although transfer functions varied for different equipment settings and for different wave conditions, they remained essentially linear over the desired frequency range.

Increasing phase shift with frequency is attributed, in part, to the slight separation distance between shaft sensor wires and the stationary wave gage. As frequency is increased, wavelength decreased

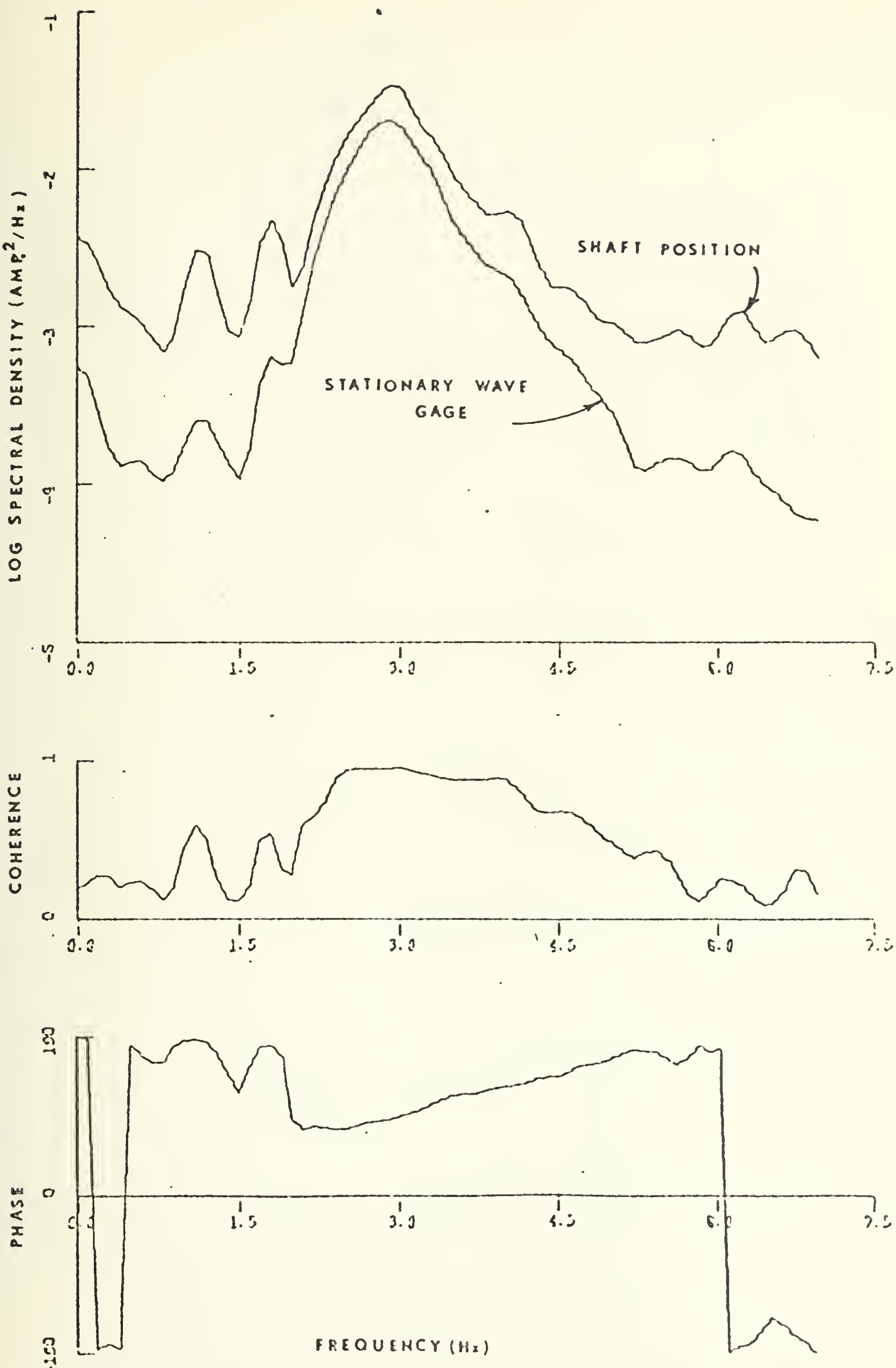

Figure 41. Broad Frequency Band, Wind Wave Exp., Two Fans

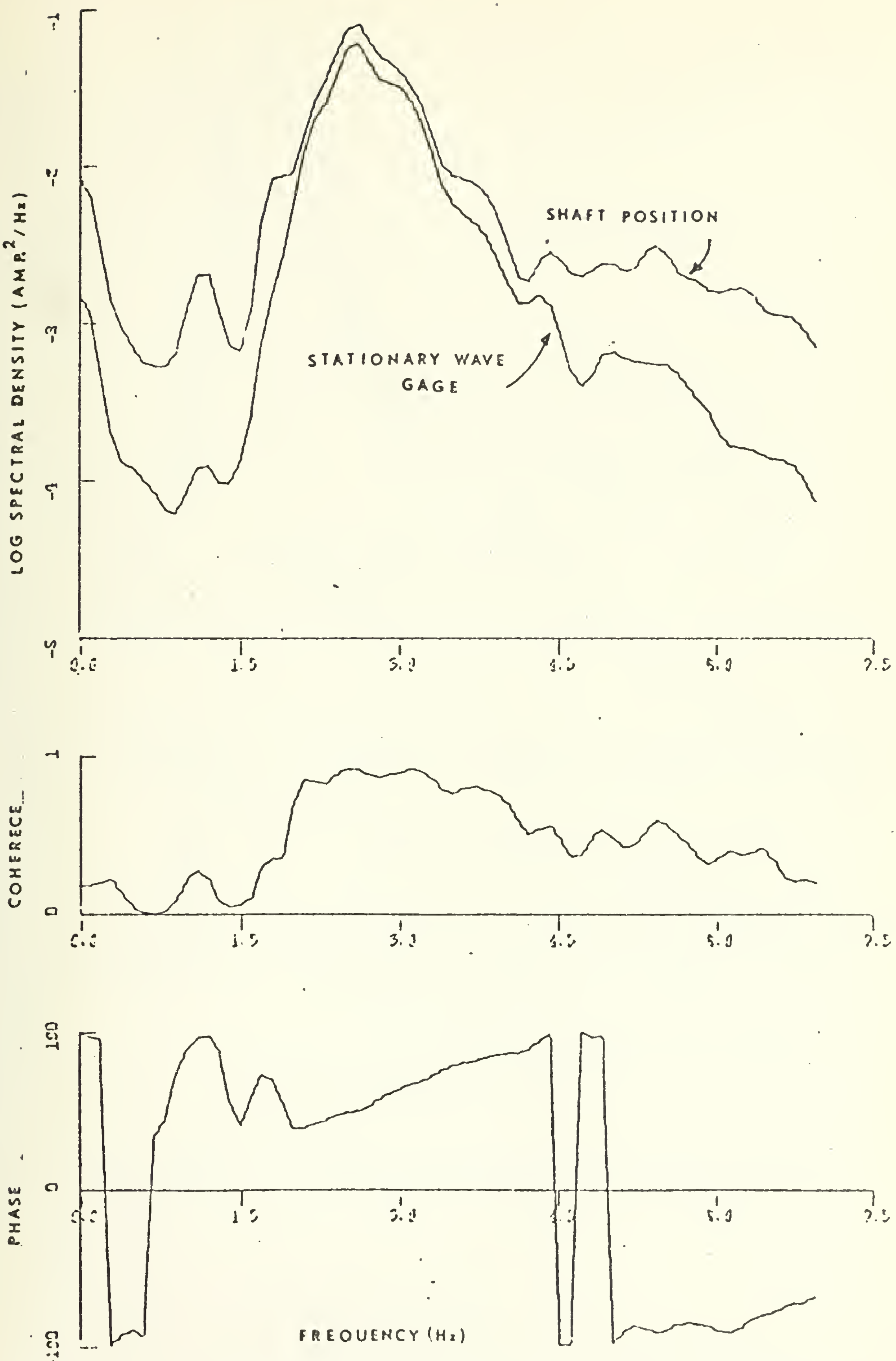

Figure 42. Broad Frequency Band Wind Wave Exp., Three Fans

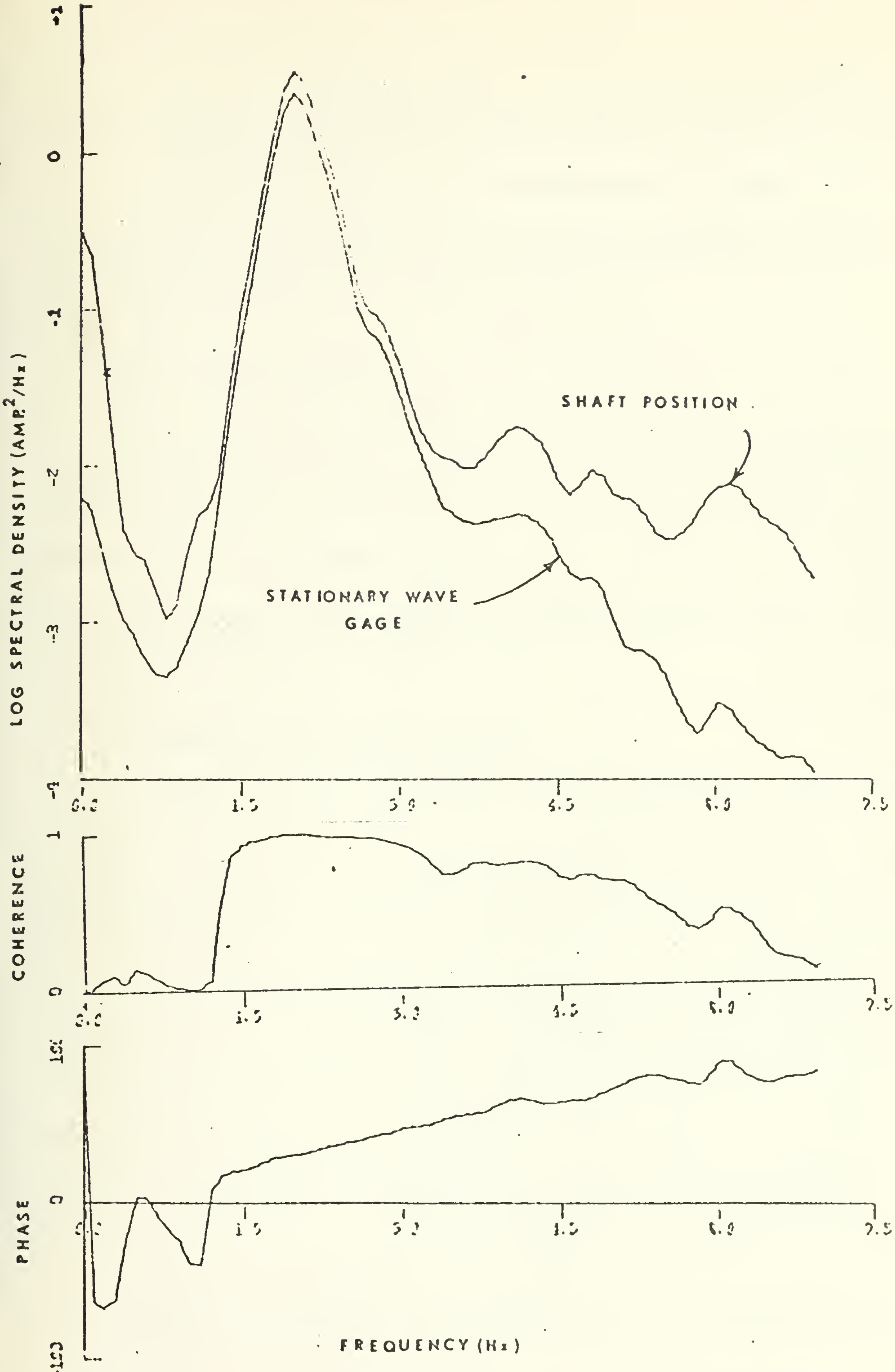

Figure 43. Broad Frequency Band Wave Exp., Five Fans

and, as a result, the apparent phase shift increased. The similar linear increase in phase angle with increasing frequency in all three experiments supports this conclusion. Spacing between the shaft sensor probes and stationary wave gage also contributed to differences in power spectra and to reduced coherence at higher frequencies.

C. FIELD EXPERIMENTS

Testing of LOWFER in the field was accomplished utilizing support equipment and research facilities aboard the Naval Postgraduate School's research vessel R/V Acania. Experiments were conducted in two phases -- those using a spar buoy to support LOWFER and those using a catamaran buoy for the supporting vehicle.

1. Spar Buoy Ocean Experiment

The spar buoy ocean experiment was conducted on the morning of July 3, 1975 at an ocean station three miles north of Lover's Point in Monterey Bay. Wind was 290°T, 5 knots; skies were clear. Ocean swell had a predominant period of 12 seconds, a 2 m swell height and was from 280° T. In the first test, a steel cable from the ship's hydrowinch was passed through a block supported by a crane and threaded through the spar buoy. A two hundred pound weight was then attached to the terminal end of the cable to hold the buoy in a near vertical attitude (figure 44). The rig with LOWFER installed was placed in the water. Support technicians in a Boston Whaler came alongside and

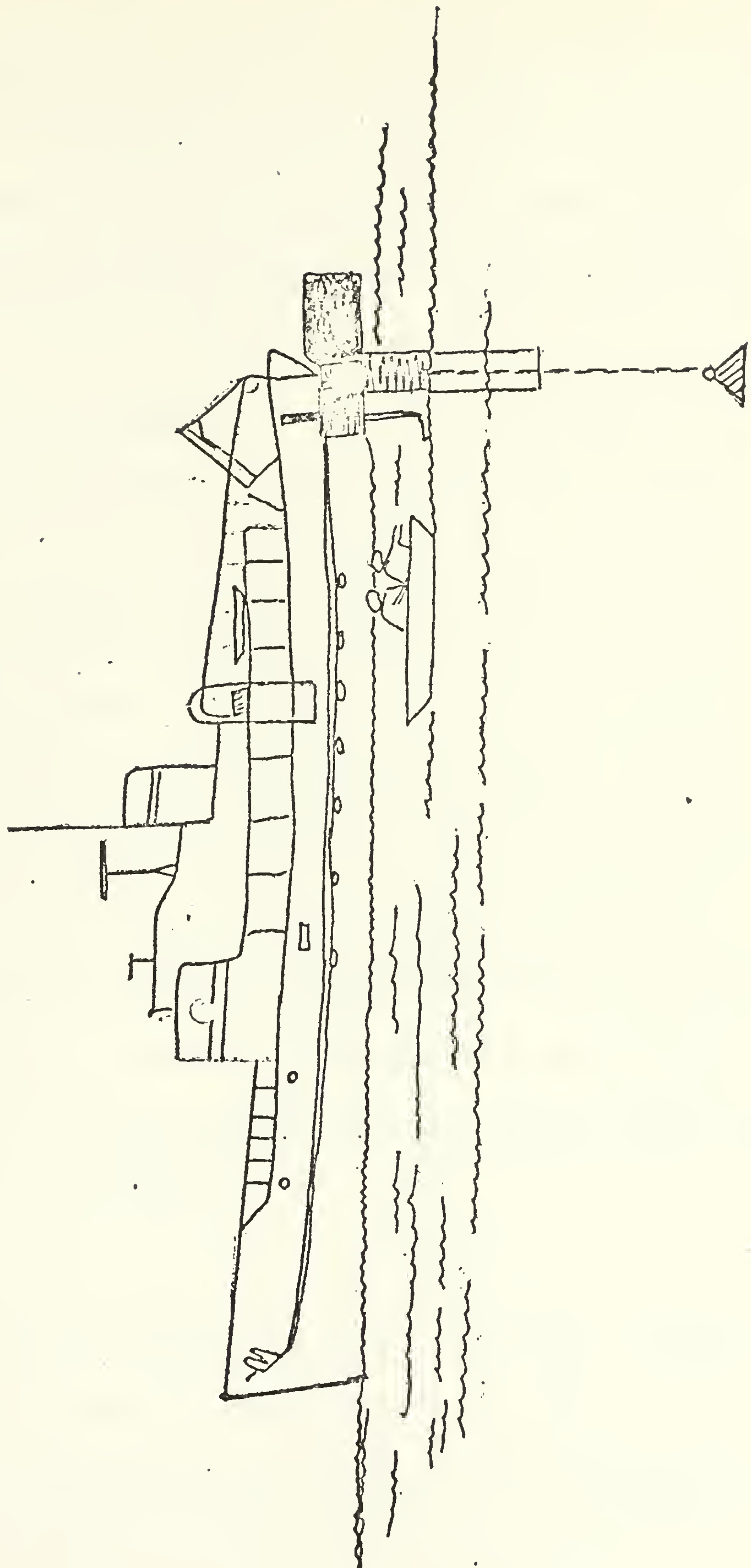

Figure 44. Spare Buoy/Wind Vane Experiment

attempted to lower the probe sensor to the water surface. Wave action made keeping the probe at the surface until power could be applied to the servo motor virtually impossible. Use of the remote Up/Dn switch on the wave follower electronic panel proved equally infeasible as proper operation depended on good communication with the Boston Whaler crew. This was not provided for during the experiment. The relatively high amplitude swell along with a virtual lack of wind (needed for stable orientation) caused a wallowing and a generally eratic heaving and pitching motion of the spar buoy. The buoy heave was often out of phase with the swell and resulted in sea water getting into the electrical connection area inside the wind vane. The large mass above the waterline (87 kg) added to the general instability. In addition, because of the spar buoy's close proximity of Acania's port quarter, the Boston Whaler crew was hampered from maneuvering to more advantageous positions. And lastly, and perhaps of greatest ultimate significance, a substantial wave diffraction pattern around the spar buoy contaminated the wave structure in the vicinity of the shaft probes. For these and for safety reasons, the experiment was terminated.

a. Results

From the experience gained in this test, troublesome areas were pinpointed and plans formulated for their solution. Solutions centered around the design of a buoy that would overcome the deficiencies of the spar configuration -- those problems associated with buoy heaving,

buoy stability, and with the formation of the diffraction pattern around the buoy. The catamaran/neutral buoyancy cylinder design resulted (figure 28).

2. Catamaran/Neutral Buoyancy Cylinder Experiments

Field experiments with the catamaran/neutral buoyancy cylinder were conducted in two separate phases. In the first experiment, procedures for deployment of the buoy were developed and low amplitude tracking runs with the wave follower recorded. In the second phase, wave follower measurements were made in moderate wave conditions in the open ocean (figure 45)

a. Phase One, Inner Harbor Experiment

Phase one was conducted in the inner harbor of the city of Monterey, Ca. alongside R/V Acania which was tied up to the pier. The first part of the experiment was devoted to the developing of buoy launching techniques and crew coordination so that LOWFER could be properly used in the ocean environment. Crew members and equipment aboard R/V Acania along with additional technical support including a Boston Whaler and crew were utilized.

Launching of the buoy was easily accomplished using preconceived plans and procedures. Once the buoy was in the water and clear of the ship, the wave follower was mounted on the buoy and the tether and electrical cable passed back to Acania and connected to proper equipment. Power was then applied to LOWFER and a wave tracking run

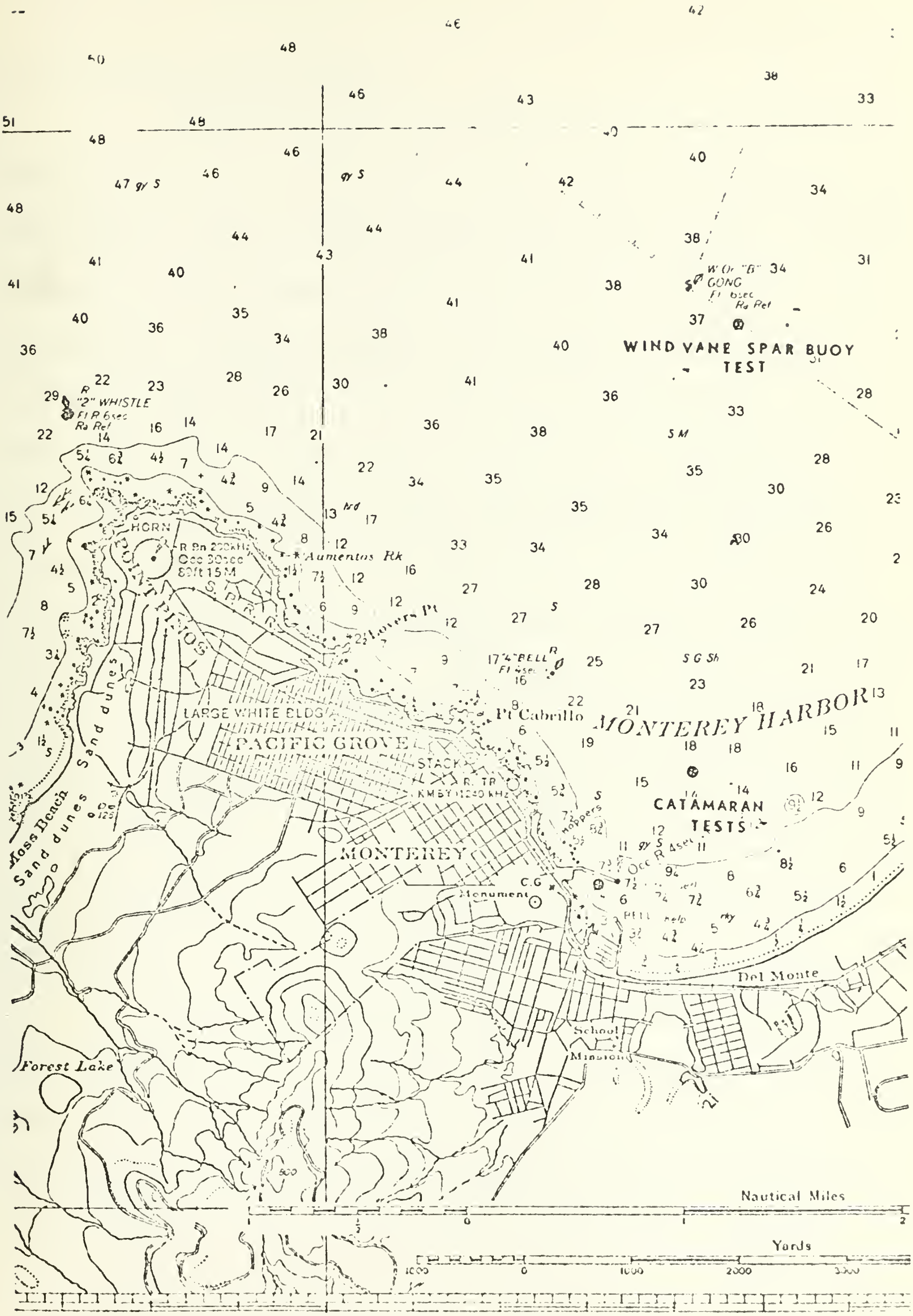

Figure 45. Ocean Test Sites

commenced. Visual operation of the system appeared normal and was, in all respects, as anticipated.

Tracking runs were conducted for ten minutes duration. Shaft position output signals were recorded on both a Sangamo 14 channel tape recorder and on a Brush 8-channel strip chart recorder. A typical segment of the strip chart recording of the shaft position output reveals adequate wave tracking by LOWFER but includes an unexpected 6 Hz component superimposed on the actual wave height (figure 46). Post-experiment analysis indicates the component to be, most likely, the result of improper adjustment of the Error Adjust and/or Reference Balance controls or an unwanted signal generated by the Sangamo tape recorder. Techniques for establishing proper equipment settings in the field will have to be devised when actually employing LOWFER in air-sea interaction studies. The energy density spectrum of the shaft position output was produced utilizing a Honeywell 96 tape recorder and a Federal Scientific Ubiquitous spectrum analyzer. It contains significant energies at 0.3 Hz, 0.56 Hz, and, 1.5 Hz (figure 47). The equipment injected energy spike at 6 Hz has been suppressed using a 0-5 Hz low pass filter.

During the experiment, visual observation of buoy characteristics including balance, heave, pitch, and on the development of a wave diffraction pattern were carried out. The buoy proved well balanced and exceptionally stable. Heave was effectively damped by the neutral buoyancy cylinder and pitch was adequately controlled by the catamaran

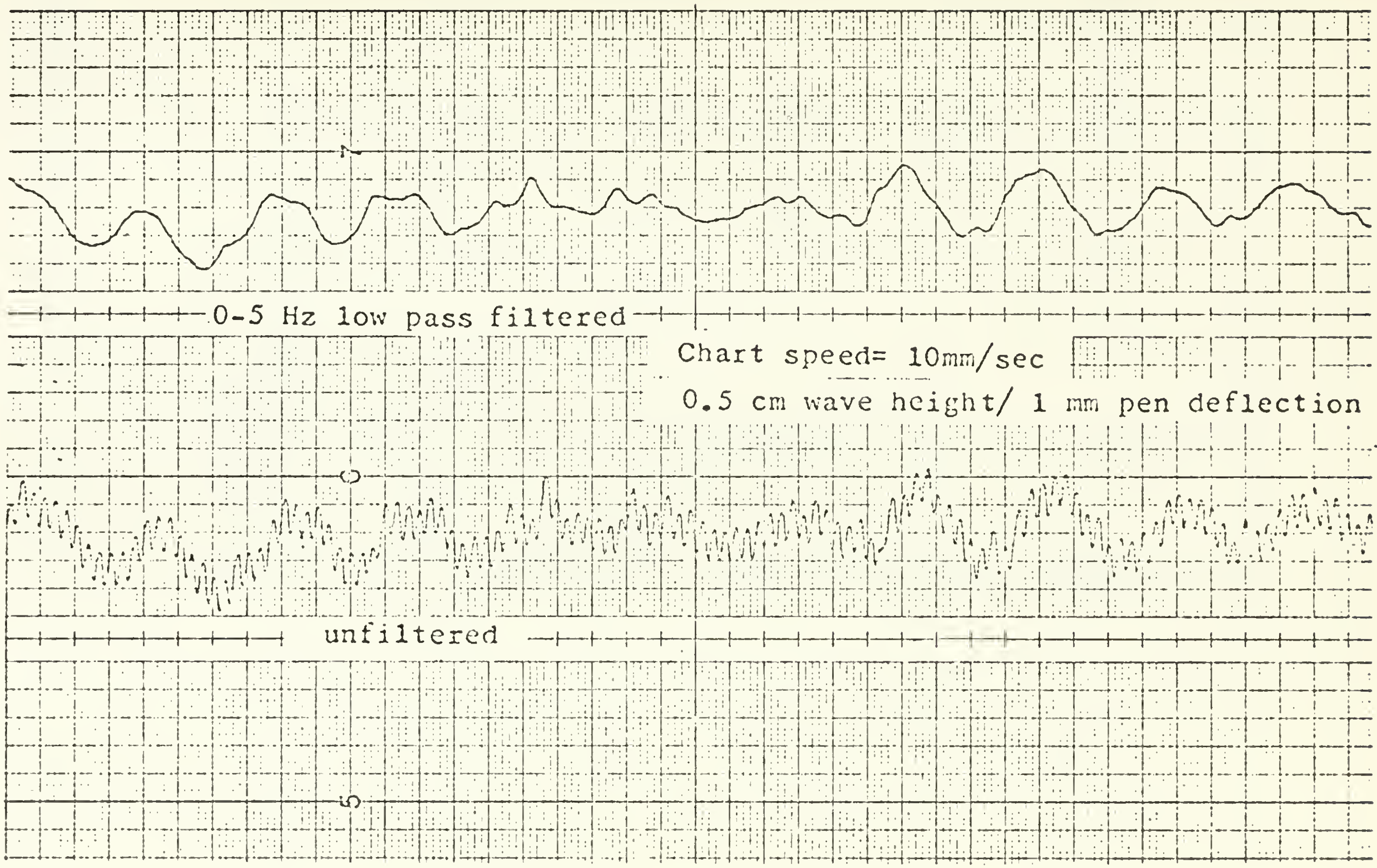

Figure 46. Inner Harbor Test, Shaft Position Output Signal

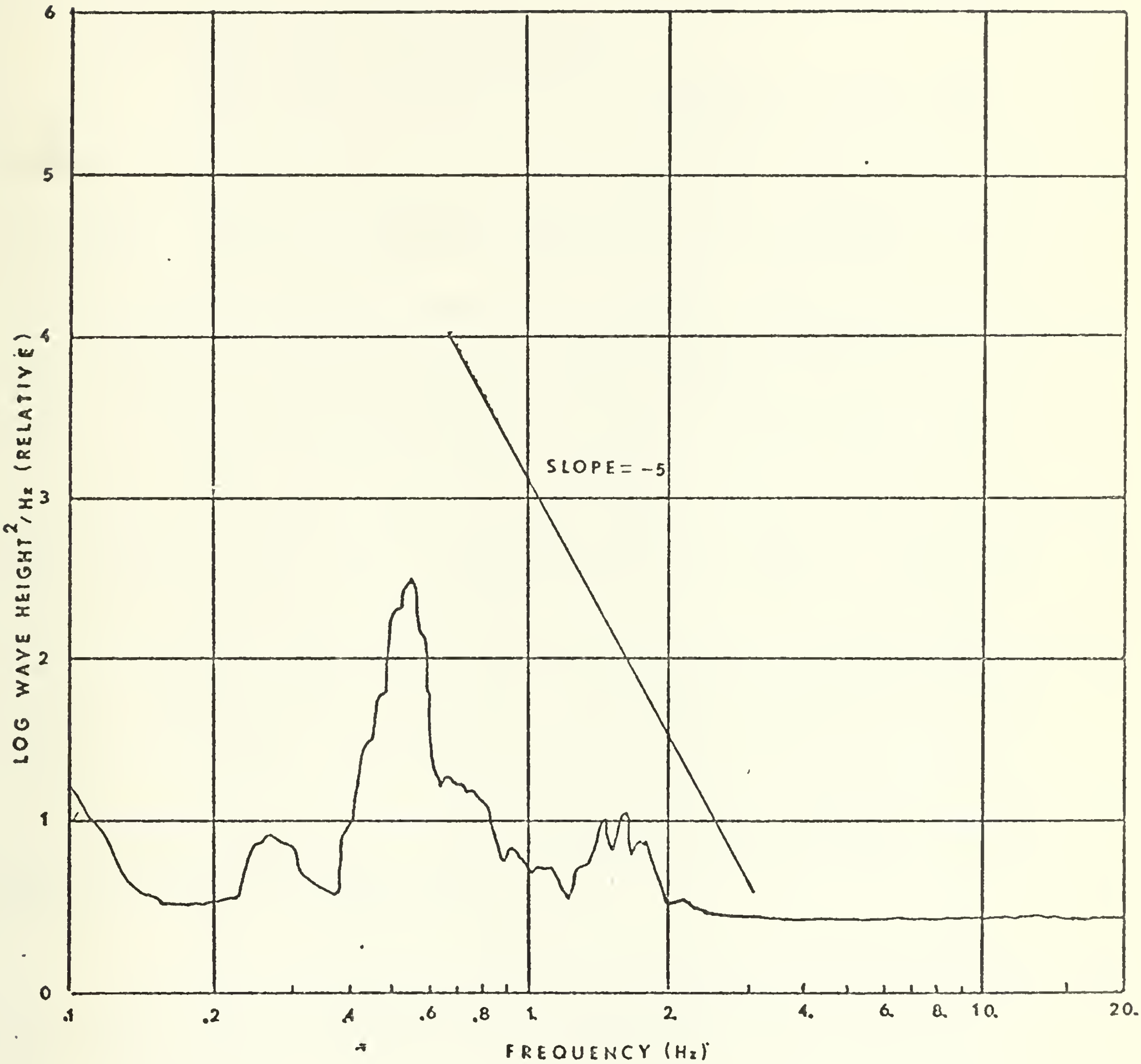

Figure 47. Inner Harbor Test, Shaft Position Output Spectrum

pontoons and righting arm. It oriented itself properly into the wind. No diffraction pattern in the vicinity of the wave follower probe could be detected.

b. Phase Two, Bay Experiment

Phase Two was conducted at a location one mile off the Monterey, California harbor breakwater (figure 45). Water depth was 17 fathoms. Observed swell was from 280°T, 1.5 m in height, and had a dominant period of approximately four seconds. The buoy was rigged with LOWFER in a manner identical to that in Phase One. Wave tracking runs of ten minutes duration were recorded. Shaft position output recordings clearly show increased wave heights and the 4 Hz predominant swell frequency (figure 48). It should be realized, however, that measured wave height is substantially less than actual wave height because of the wave following effects of the buoy. An energy spectrum of the shaft position output yields significantly higher energies at lower frequencies. The equipment injected 6 Hz signal is, again, present although reduced somewhat in amplitude (figure 49).

Buoy performance was again excellent in the higher wave conditions. There were times however when the probe of the wave follower was pulled from the water surface (figure 50). The condition was observed only when sharp crested waves passed under the buoy. Those portions of the shaft position output trace that have a straight line appearance are indicative of when the probe is not in contact with the

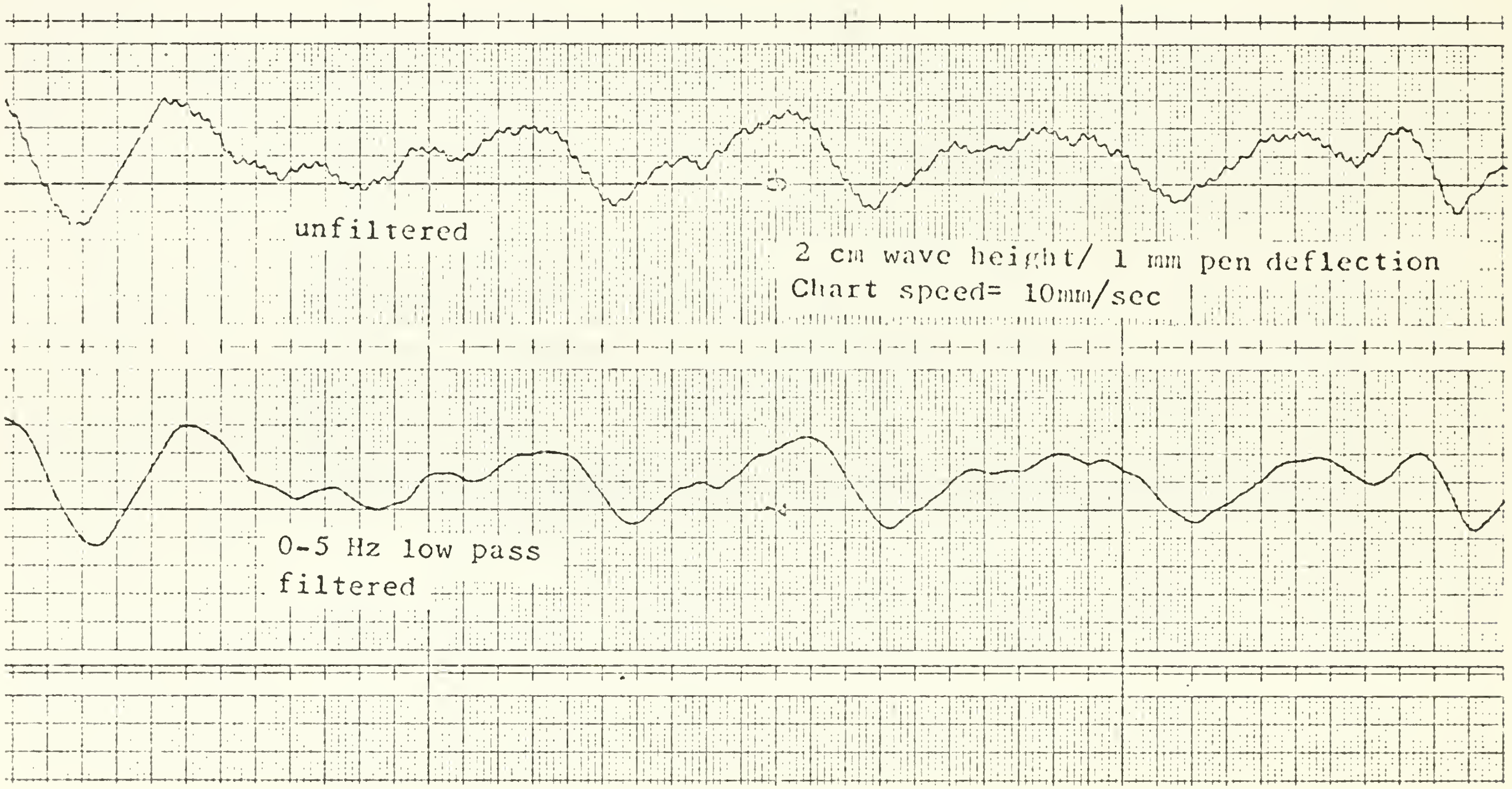

Figure 48. Bay Test, Shaft Position Output Signal

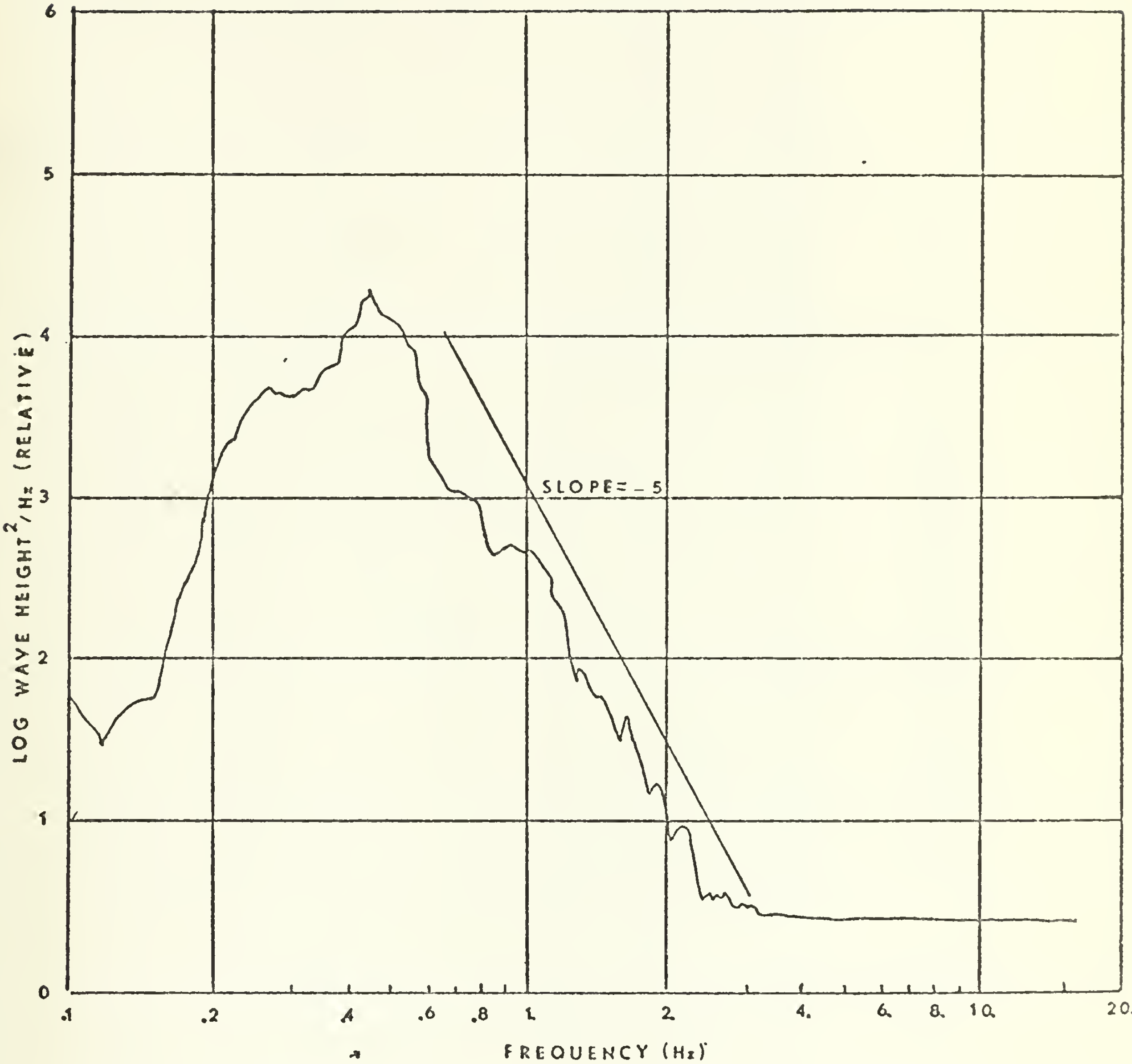

Figure 49. Bay Test, Shaft Position Output Spectrum

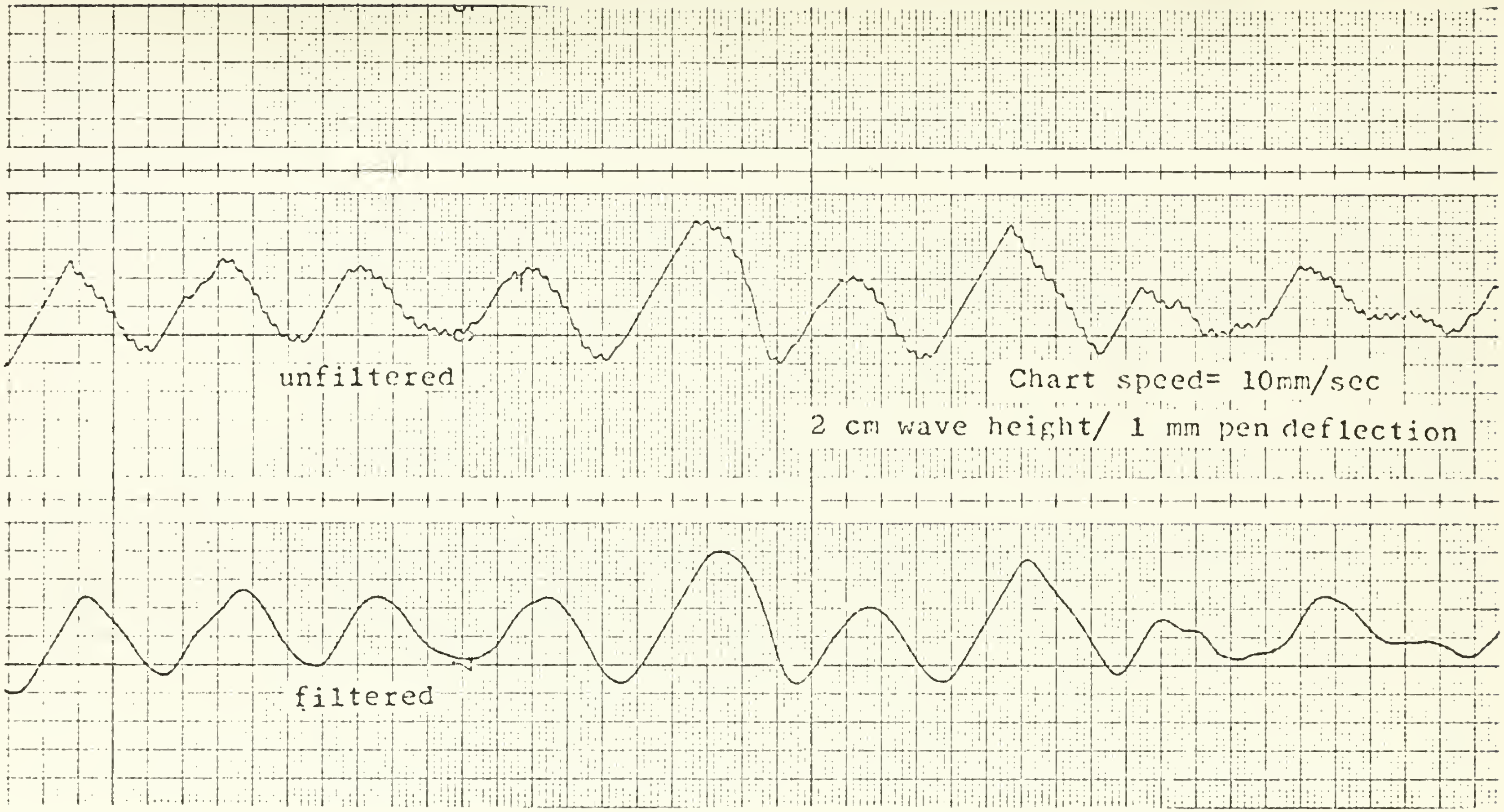

Figure 50. Bay Test, Shaft Position Output When Probe Is Pulled Free from Sea Surface

surface. Visual observations of tracking by the probe sensor rarely detected this phenomenon indicating the probe was, at all times, actually following very closely the water surface.

V. CONCLUSIONS

The Lindquist Ocean Wave Follower has the capability of accurately following a wide range of wave conditions both in the laboratory and in the field. In a narrow frequency band wave regime, maximum observed LOWFER error tracking was 7% or less than most runs having errors of 3 percent or less. Tracking error is dependent upon wave height, wave frequency and wave shape. Close agreement between the shaft position signal output spectrum and the stationary wave gage spectrum was observed during the wind-generated broad frequency band experiments. LOWFER has a useable frequency response range of 0-4 Hz. However, to realize acceptable accuracies, careful adjustment of the wave follower is necessary. This has proven to be difficult in both wind-generated wave laboratory experiments and in those conducted in the field.

It has also been shown that LOWFER can be adapted for use in the ocean environment. However, by using a buoy system to follow large waves, some means of reconstructing the actual wave spectrum must be devised. A three-dimensional accelerometer system mounted on the buoy would give overall motion of the buoy. Methods of converting measurements to a reference frame based on this motion could then be developed. In addition, instrumentation for measurement of the wind velocity vector should be incorporated. Thus far, the discussion

presupposes that buoy motion can contaminate or mask critical turbulence measurements. However, the system does offer the possibility of taking near surface turbulence measurements in exceedingly high wave conditions heretofore unsampled. It may be that significant information can be retrieved in high sea states despite buoy motions.

The use of a buoy as a second stage appears to have advantages over fixed mounted wave followers. Perhaps foremost is the fact that the buoy is free to be positioned at any desired location under a wide range of wave conditions thus enabling measurements to be taken during the entire growth process of wave development. Use of a tethering cable allows instrumentation to be remotely positioned from the actual sensors as, for example, on the R/V Acania during the field portion of the project. The ability of the buoy to orient itself in the direction of the mean wind velocity vector and thus keep sensors directed into the wind is also considered an advantage. Finally the relatively low cost of buoy construction and operation most likely will make a two stage buoy system more cost effective than fixed mounted systems.

Disadvantages of the buoy again center around unwanted motion that will have to be removed or compensated for during data analysis. The probable increase in the use of computer time as a result of this will have to be weighed against using alternate or fixed mounted wave follower systems. It is not known at this time what effects the buoy will

have on the wind field, but in light of its small profile 966 cm^2 (150 in^2) and the forward position of the wave follower with respect to the buoy, it is suspected that they can be disregarded. Optimization of the wave follower tracking ability has also been troublesome and techniques will have to be developed to overcome this.

VI. RECOMMENDATIONS

It is recommended that a follow-on program of testing be instituted to develop ways of optimizing the LOWFER prior to employment in the ocean environment. In addition, a program to determine the effects of buoy motion on turbulence measurements would enable investigators to make comparisons between fixed-mounted wave followers and a two-stage buoy/wave follower system. If necessary, data could be transformed into a stable reference system with the opportunity then to extract meaningful information regarding phenomena at the air-sea interface.

BIBLIOGRAPHY

1. Bub, F. L., Surf Zone Wave Kinematics, Master's Thesis, U. S. Naval Postgraduate School, Monterey, California, 1972.

2. Davis, G. M., Measurement of Air Temperature and Wind Velocity from One to Eighty Meters above the Sea Surface, Master's Thesis, Naval Postgraduate School, 1969.

3. Kinsman, B., Wind Waves, Their Generation and Propagation on the Ocean Surface, Prentice Hall, Englewood Cliffs, N. J., 1970.

4. Lai, R. J. and Shemden, O. H., Laboratory Investigation of Air Turbulence above Simple Water Waves, Journal of Geophysical Research, Vol. 76, No. 30, p. 7334-7350, 20 October, 1971.

5. Lindquist, D., Ocean Wave Follower, Unpublished Manuscript, July 1974.

6. Office of Naval Research, Technical Report Number 3, A System for the Generation and Measurement of Capillary-Graviety Waves, McGoldrick, L. F., University of Chicago, August, 1969.

7. Chesapeake Bay Institute, Technical Report Number 58, Chesapeake Bay Institute Wave Follower, Peep, M. and Flower, J., 1969.

8. Ramzy, J. R., and Young, E. T., Jr., Investigation of Temperature Fluctuations Near the Air-Sea Interface, Master's Thesis, Naval Postgraduate School, 1968.

9. Coastal Engineering Center, University of Florida, Technical Report Number 18, Investigation of the Velocity Field over Waves Using a Wave Follower, Shemden, O. H. and Lai, R. J., 1973.

10. Stewart, R. H., Laboratory Studies of the Velocity Field over Deep Water Waves, Journal of Fluid Mechanics, Vol. 142, Part 4, p. 733-754, 1970.

11. Stewart, R. H., Comments on Paper by R. J. Lai and O. H. Shemden'Laboratory Investigation of Air Turbulence above Simple Water Waves', Journal of Geophysical Research, Vol. 77, No. 30, 20 October 1972.

DISTRIBUTION LIST

		No. Copies
1.	Department of Oceanography, Code 58 Naval Postgraduate School Monterey, CA 93940	3
2.	Oceanographer of the Navy Hoffman II 200 Stovall Street Alexandria, VA 22332	1
3.	Office of Naval Research Code 480 Arlington, VA 22217	1
4.	Dr. Robert E. Stevenson Scientific Liaison Office, ONR Scripps Institution of Oceanography La Jolla, CA 92037	1
5.	Library, Code 3330 Naval Oceanographic Office Washington, D.C. 20373	1
6.	SIO Library University of California, San Diego P. O. Box 2367 La Jolla, CA 92037	1
7.	Department of Oceanography Library University of Washington Seattle, WA 98105	1
8.	Department of Oceanography Library Oregon State University Corvallis, Oregon 97331	1
9.	Commanding Officer Fleet Numerical Weather Central Monterey, CA 93940	1

10.	Commanding Officer Environmental Prediction Research Facility Monterey, CA 93940	1
11.	Department of the Navy Commander Oceanographic System, Pacific Box 1390 FPO San Francisco 96610	1
12.	Defense Documentation Center Cameron Station Alexandria, VA 22314	2
13.	Library (Code 0212) Naval Postgraduate School Monterey, CA 93940	2
14.	Mr. David Lindquist 4648 West 14 Ave. Vancouver, British Columbia Canada VGR 2Y6	1
15.	Dr. Edward B. Thornton Department of Oceanography Naval Postgraduate School Monterey, CA 93940	1
16.	Dr. Noel E. J. Boston Department of Oceanography Naval Postgraduate School Monterey, CA 93940	2
17.	Mr. Woodrow Reynolds Department of Oceanography Naval Postgraduate School Monterey, CA 93940	1
18.	LT John W. Bonnett 275 J Ave. Coronado, CA	2
19.	Mr. Edward N. Bonnett 110 Hartle Road Glenshaw, PA 15116	1

Thesis
B682
c.1
163157
Bonnett
Analysis of the Lindquist ocean wave follower.